PRINCETON PLASMA PHYSICS LABORATORY

Core-Edge Integrated Gyrokinetic Simulations of Fusion Plasmas

Presenter name: Julien Dominski

PPPL	J Dominski, CS Chang, R Hager, S Ku, F Parra, T Barbui, LF Delgado
Jubilee Development	A Scheinberg
CEA-IRFM	P Maget, P Manas, J Morales, and WEST team
ADAS team at UKAEA	M O'Mullane
IPP Garching and U. Seville	A Kallenbach, T Putterich, E Viezzer, and AUG team
Argonne National Laboratory	V Mateevitsi, and ANL Visualization Team

ITER summer school, June 30th-July 4th 2025, Aix-en-Provence

Plan

1. Introduction on modeling a fusion reactor

   An energy amplifier subject to transport losses and impurity radiation

2. Gyrokinetic modeling of heat and particle confinement

   Collisional & turbulent transport, GK equation, delta-f & total-f, local & global

3. Atomic physics of tungsten and low-Z impurities

   Ionization/recombination coupled to the transport, and radiation

4. Applications to WEST and ASDEX-U plasma

Integrated modeling of a tokamak

As addressed by Lawson (1957), an efficient fusion reactor must provide **at least** as much electric power as it consumes.

The amplification factor is $Q = (P_{out} + P_\alpha)/P_{aux}$
- $Q = 1$ ignition
- $Q = 10$ is ITER goal (maximum by JET is 0.67)
- $Q = \infty$ is the combustion (no heating is needed)

The confinement time τ evaluates how fast the total plasma energy W is lost due to transport.

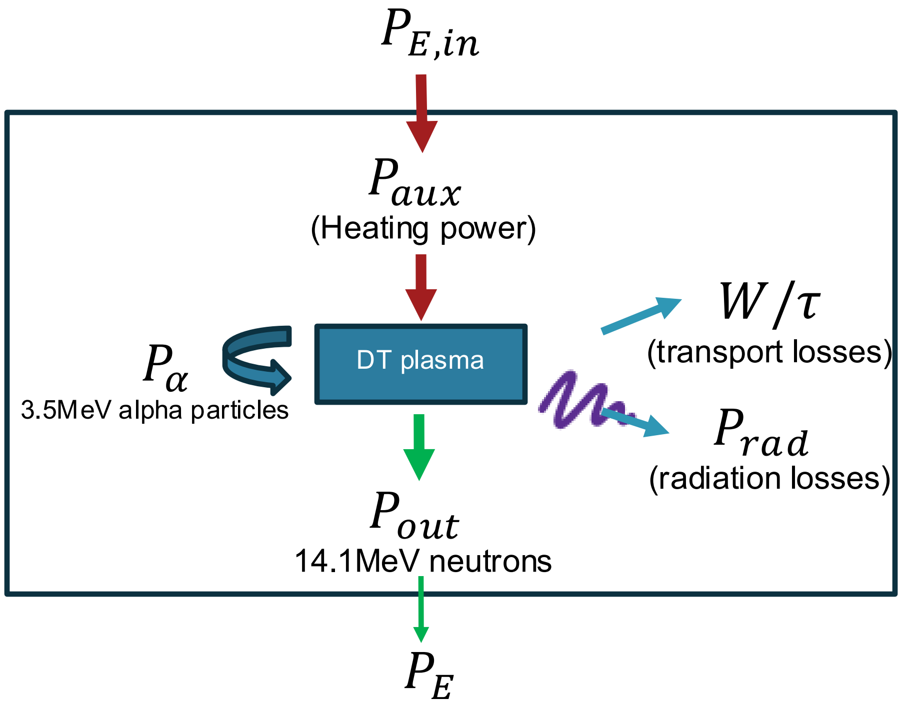

Lawson J. (1957) *"Some criteria for a power producing thermonuclear reactor"*

https://www.iter.org/node/20687/tao-q

Integrated modeling of a tokamak

As addressed by Lawson (1957), an efficient fusion reactor must provide **at least** as much electric power as it consumes.

The amplification factor is $Q = (P_{out} + P_\alpha)/P_{aux}$
- $Q = 1$ ignition
- $Q = 10$ is ITER goal (maximum by JET is 0.67)
- $Q = \infty$ is the combustion (no heating is needed)

The confinement time τ evaluates how fast the total plasma energy W is lost due to transport.

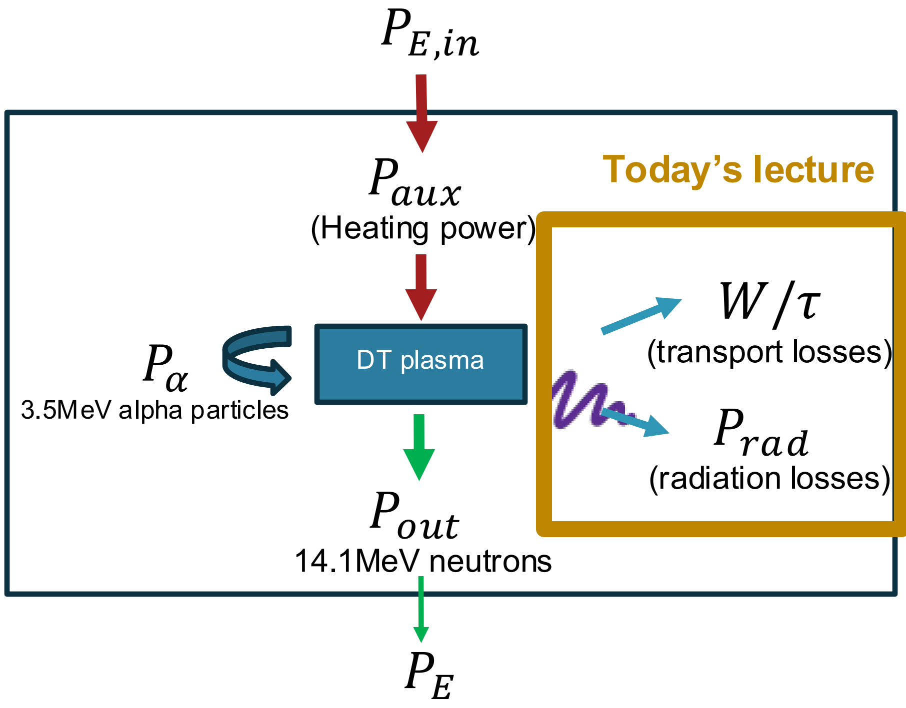

Lawson J. (1957) *"Some criteria for a power producing thermonuclear reactor"*

https://www.iter.org/node/20687/tao-q

State of the art whole device gyrokinetic modeling of an ASDEX-U H-mode plasma (4ms) with XGC
Including kinetic e- and D+ ions, as well as W, B, and He impurities.
Visualization of the full tungsten density.
Modeling the collisional and turbulent transport (W/τ) – radiation as a post-processing (for now)

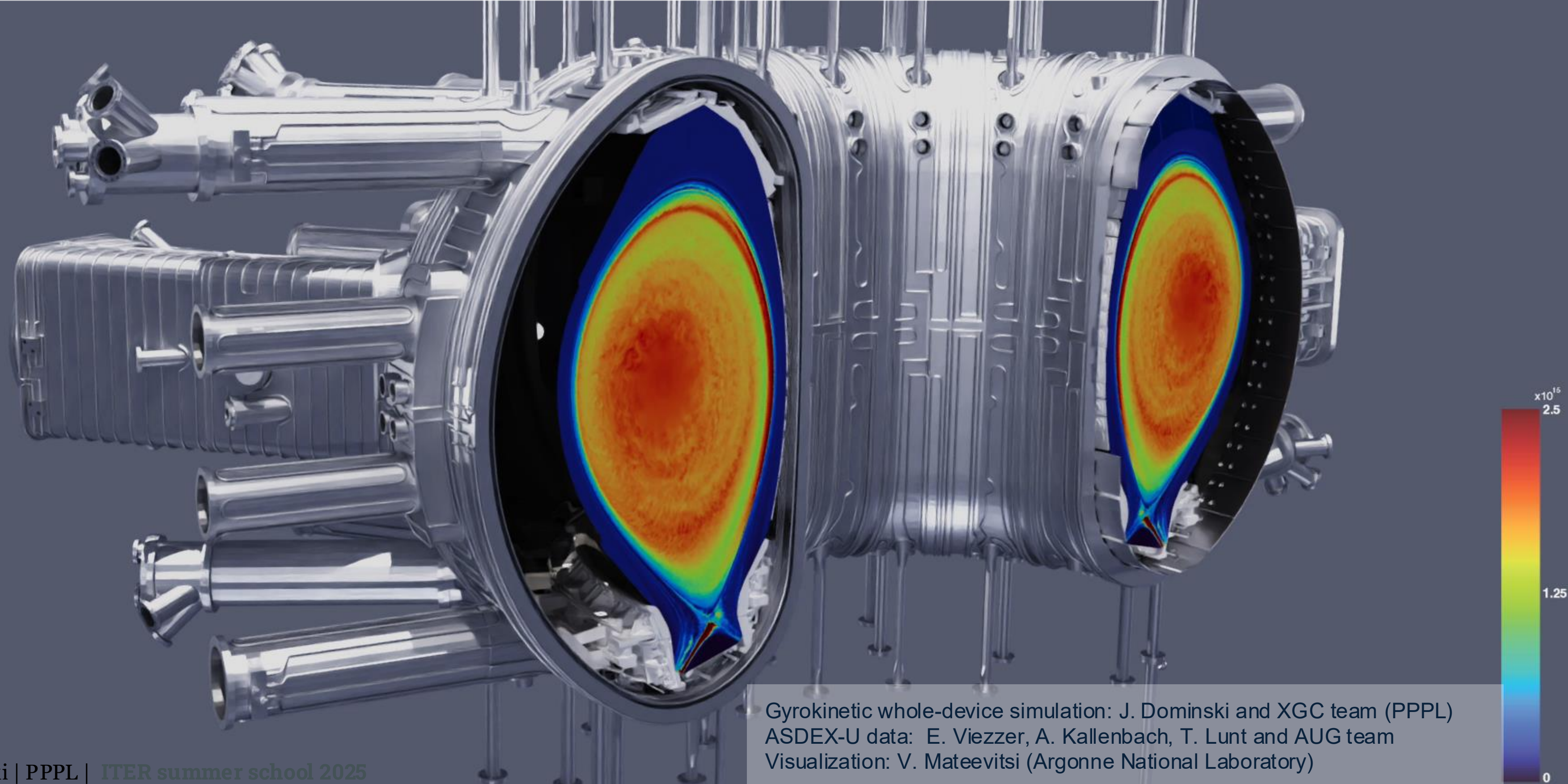

Gyrokinetic whole-device simulation: J. Dominski and XGC team (PPPL)
ASDEX-U data: E. Viezzer, A. Kallenbach, T. Lunt and AUG team
Visualization: V. Mateevitsi (Argonne National Laboratory)

Gyrokinetic modeling of fusion plasma

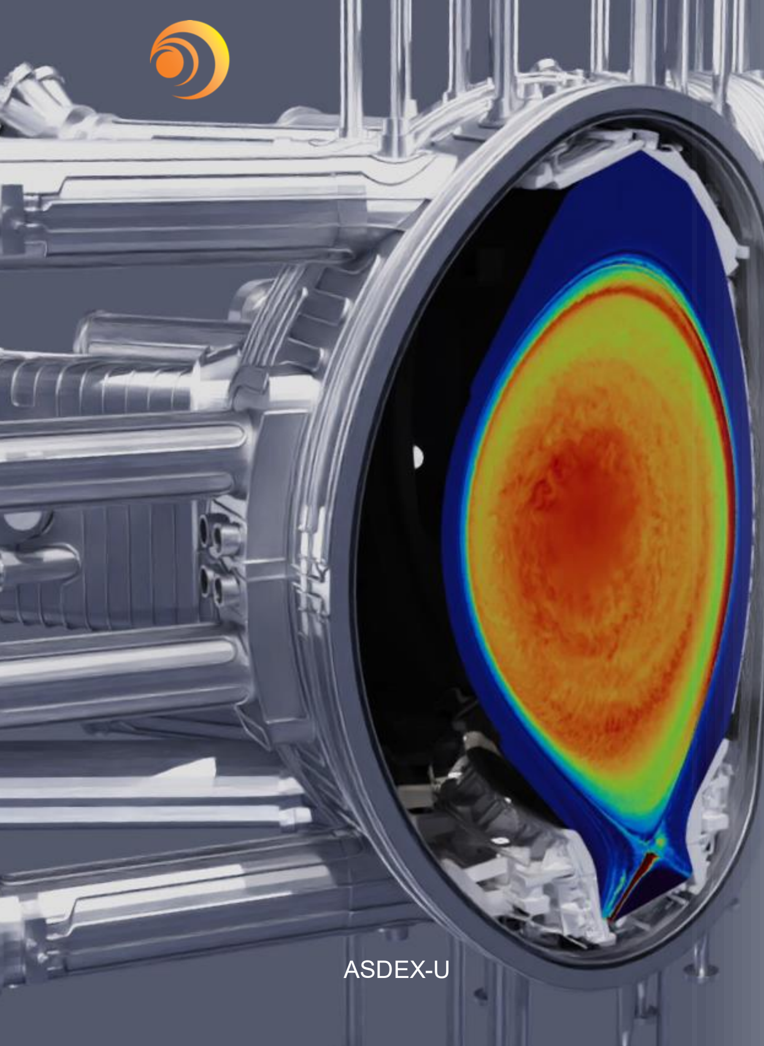

XGC a multi-species total-f gyrokinetic code covering the whole volume with X-point

- Optimized for edge diverted geometry
- Gyrokinetic model over the whole volume
- **Nonlinear Fokker-Planck collision operator**
- **Multi-impurities, bundles of tungsten**
- **Ions atomic physics** (radiation, ionization / recombination)
- Neutral recycling, rotation, heat/torque sources
- Electromagnetic RMP model
- **Exascale-ready and portable** (GPU/Kokkos/C++)

General XGC references:
S. Ku et al., Phys. Plasmas (2018)
J. Dominski et al., *J. Plasma Phys.* (2019)
R. Hager et al., Phys. Plasmas (2022)

https://xgc.pppl.gov

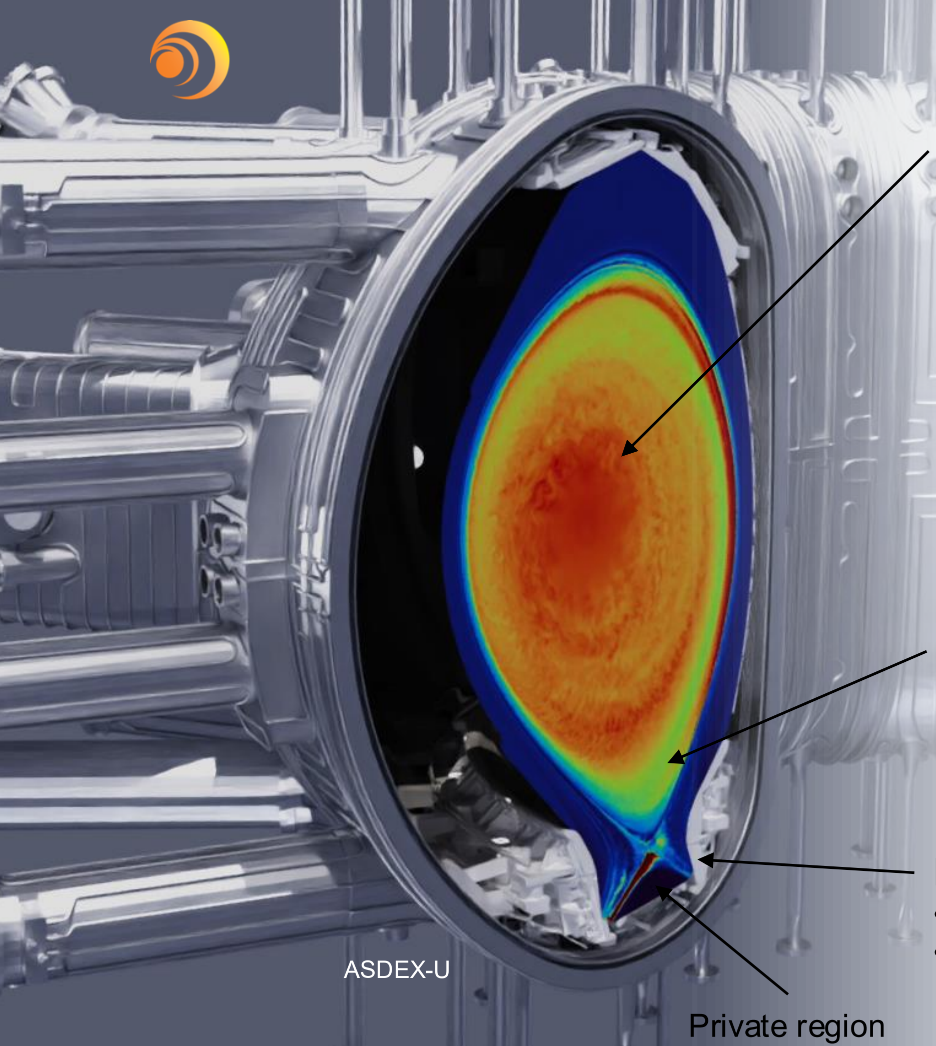

Core (burning plasma: hot and dense)

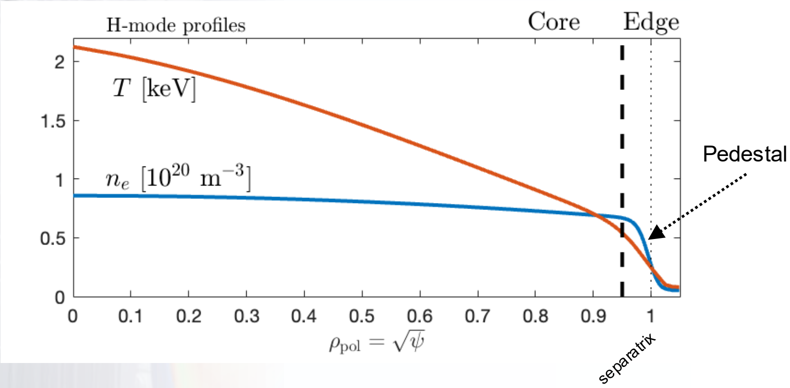

Edge region before the wall

- H-mode Pedestal: region with steep gradients
- X-point and separatrix (ψ=1)
- Scrape-off-layer (SOL): open field lines with strike points on the wall/divertor

Divertor and wall

- Heat deposition designed to strike the divertor tiles
- Source of impurities (W, C, Li,…) radiating energy

Core and edge regions

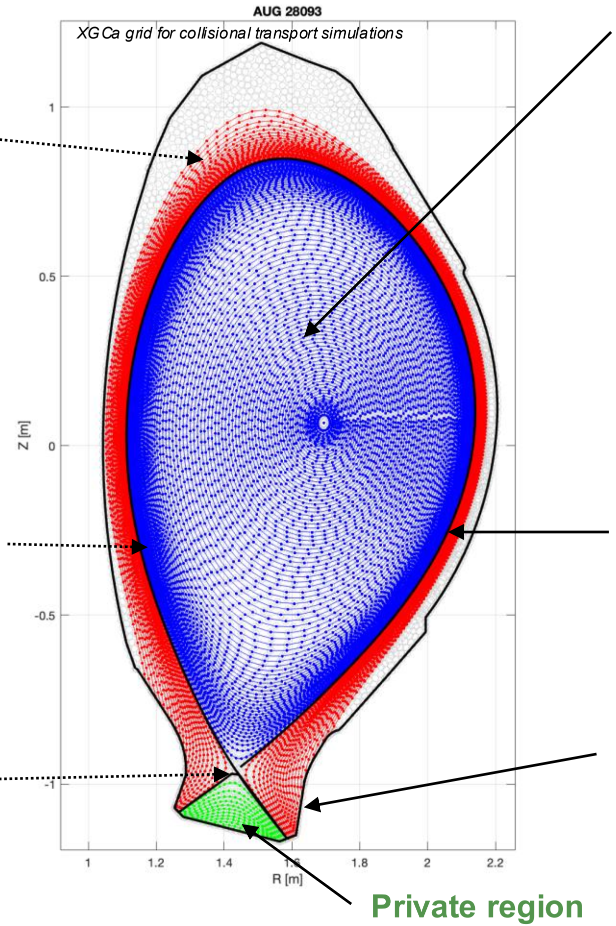

Core (burning plasma: hot and dense)

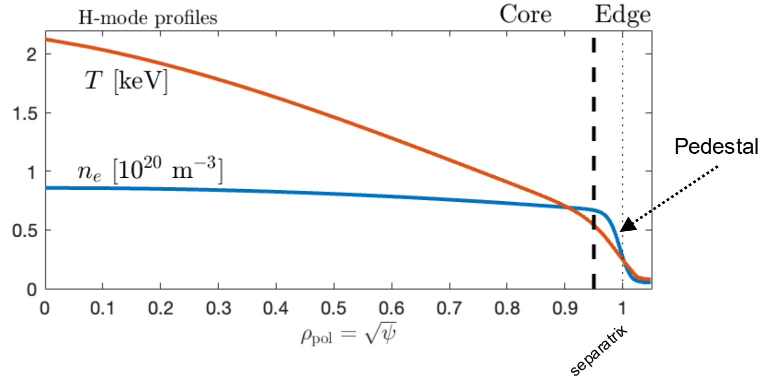

Edge region before the wall

- H-mode Pedestal: region with steep gradients
- X-point and separatrix (ψ=1)
- Scrape-off-layer (SOL): open field lines with strike points on the wall/divertor

Divertor and wall

- Heat deposition controlled to land on the divertor tiles
- Source of impurities (W, C, Li,…) : sputtered, puffed,…

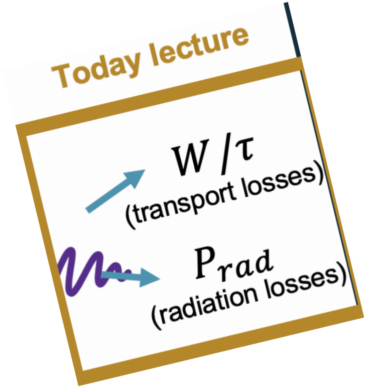

Transport modeled with gyrokinetic

- Collisional transport (~neoclassical) – 2D *axisymmetric*
- Turbulence transport (ExB drift) – *3D*

Atomic physics modeled with ADAS rates

- Ionization/recombination of the ions
- Radiation cooling of the electrons by the ions

Plan

- Introduction to gyrokinetic modeling
- Applications to tungsten modeling in WEST and ASDEX

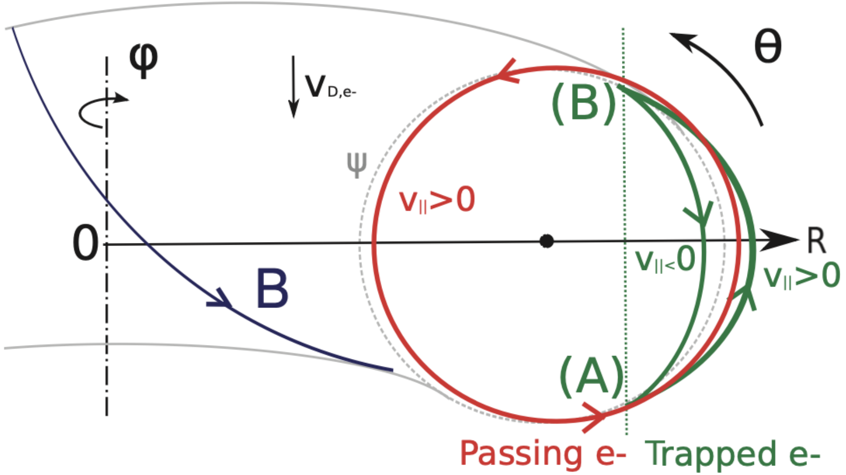

The magnetic moment, μ, being an adiabatic invariant, the magnetic energy μB varies with the magnetic field strength, B, proportionally to 1/R.

Particle lacking energy, $0.5\ mv_{||}^2 + \mu B < \mu B_{max}$, will be trapped and bounce back when $v_{||}=0$.

Particle orbits and collisional transport (2D)

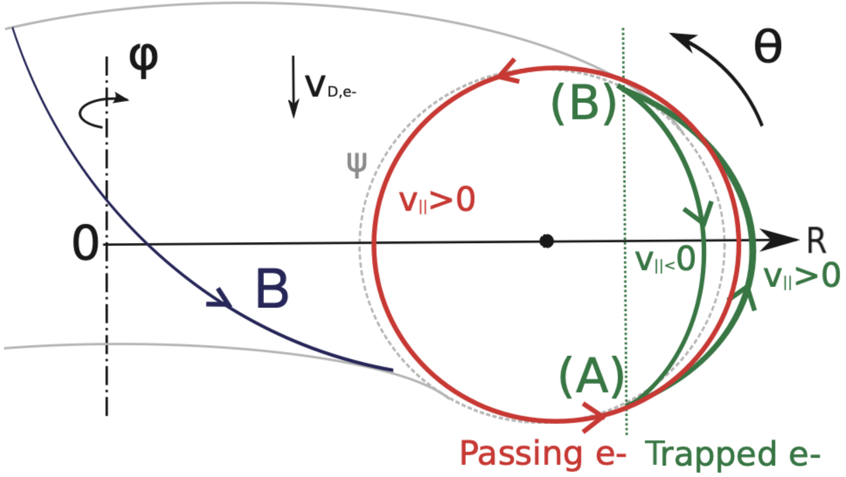

The magnetic moment, μ, being an adiabatic invariant, the magnetic energy μB varies with the magnetic field strength, B, proportionally to 1/R.

Particle lacking energy, $0.5\, mv_{||}^2 + \mu B < \mu B_{max}$, will be trapped and bounce back when $v_{||}=0$.

Collisional transport (2D) arises because collisions between particles make them change orbits.

This change of orbits corresponds to a radial step. This stochastic process leads to a diffusion.

This is the so-called neoclassical transport.

Regime	ν^*	Dominant Particle	Transport Scaling
Banana	$\nu^* \ll 1$	Trapped	$\chi \propto \nu$
Plateau	$\nu^* \sim 1$	Both	$\chi \approx$ const
Pfirsch-Schlüter	$\nu^* \gg 1$	Passing	$\chi \propto \nu$

ν^* is the ratio between collision and bounce orbit frequencies

Micro-instabilities and turbulence (3D)

Various micro-instabilities develop in magnetic fusion devices. They are field aligned ($k_\perp \gg k_\parallel$) and require a 3D modeling. Below is a fluid illustration of the ion temperature gradient (ITG).

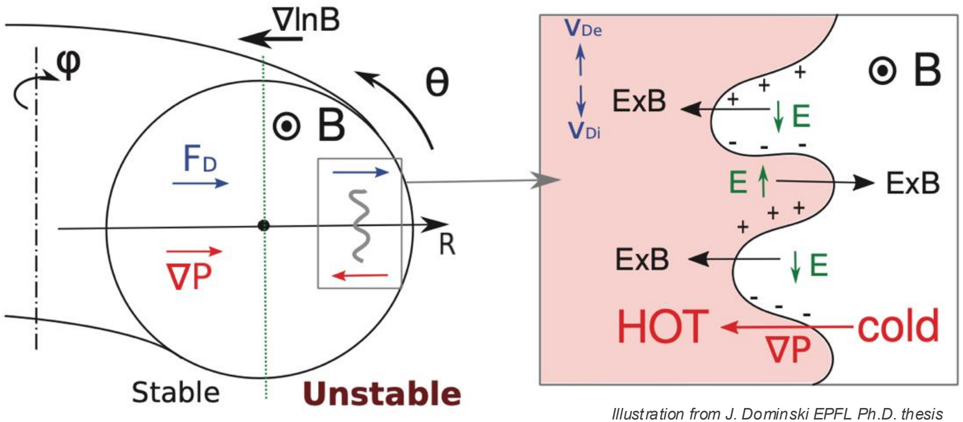

Illustration from J. Dominski EPFL Ph.D. thesis

The charge at the interface is dominated by the region of stronger drift.

- Ion and e- drifts, of opposite directions, react to a δf perturbation by perturbing the charge ($v_d . \nabla \delta f$).
- The corresponding field perturbation sustains an $E \times B$ drift that can amplify the δf perturbation.

Micro-instabilities and turbulence (3D)

Various micro-instabilities develop in magnetic fusion devices. They are field aligned ($k_\perp \gg k_\parallel$) and require a 3D modeling. Below is a fluid illustration of the ion temperature gradient (ITG).

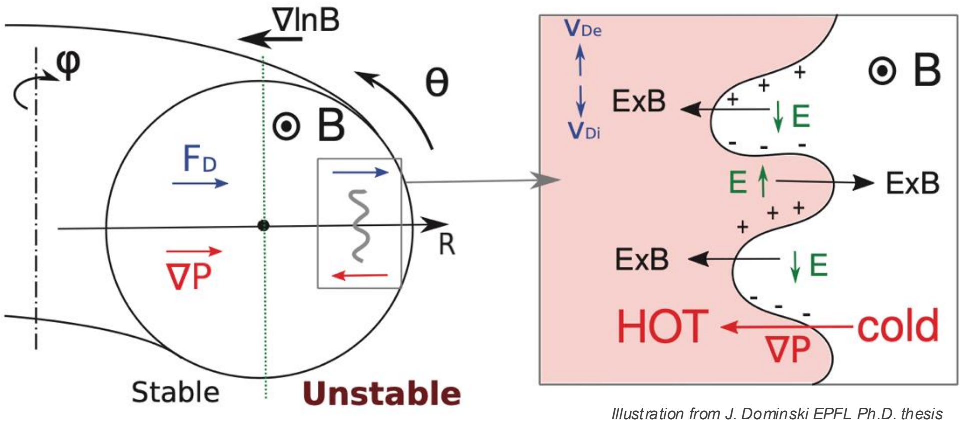

Illustration from J. Dominski EPFL Ph.D. thesis

The charge at the interface is dominated by the region of stronger drift.

- Ion and e- drifts, of opposite directions, react to a δf perturbation by perturbing the charge ($v_d.\nabla\delta f$).
- The corresponding field perturbation sustains an $E \times B$ drift that can amplify the δf perturbation.

The micro-instabilities coupled to the zonal-flow, grow until saturation. This nonlinear saturated turbulent regime sustains nonlinear turbulent fluxes of heat and particles, $v_{E\times B}\,\delta f \sim \imath k_y\,\phi^*\delta f$.

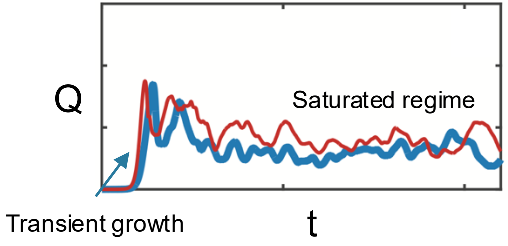

Motivation for gyrokinetic modeling

Collisional and turbulent transport can be modeled within the gyrokinetic theory.

- Particle orbits
- Collisions and associated 2D transport.
- Field equations (Poisson and Ampere) and associated 3D instabilities.
- Gyrokinetic ordering

In the edge the collisional and turbulent fluxes have similar scales, and they cannot be trivially split, as it is usually done in the core.

Gyrokinetic modeling of heat deposition

Heat load width calculation is an example of application of the XGC code to study edge tokamak physics.

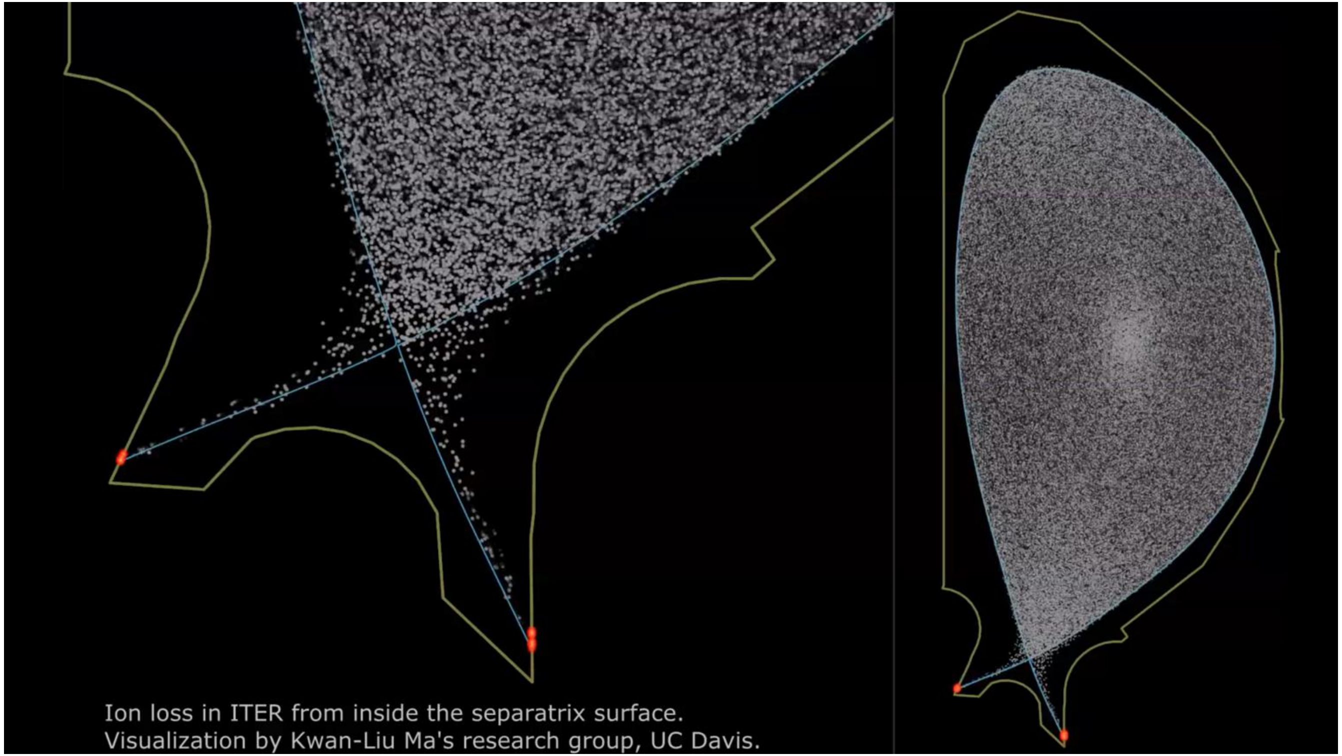

CS Chang et al. *Phys. Plasmas* 28, 022501 (2021)
C.S. Chang *et al* 2017 *Nucl. Fusion* **57** 116023

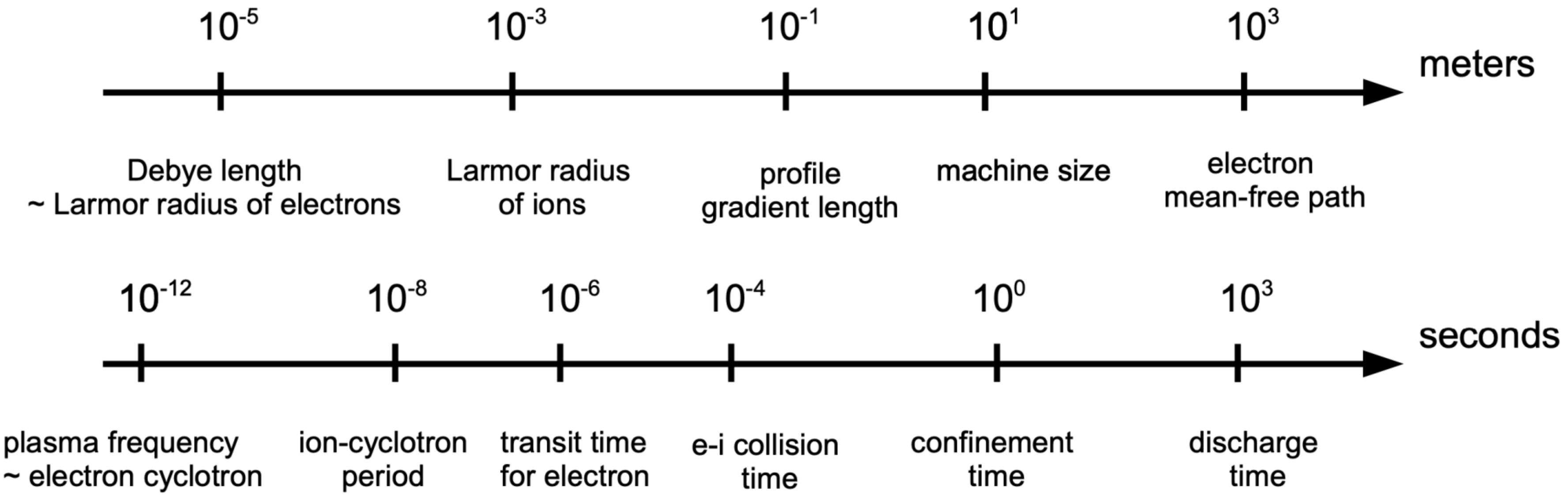

WEST record: 1337s

Long pulse of operation

Plasma scales and relevance of gyrokinetic

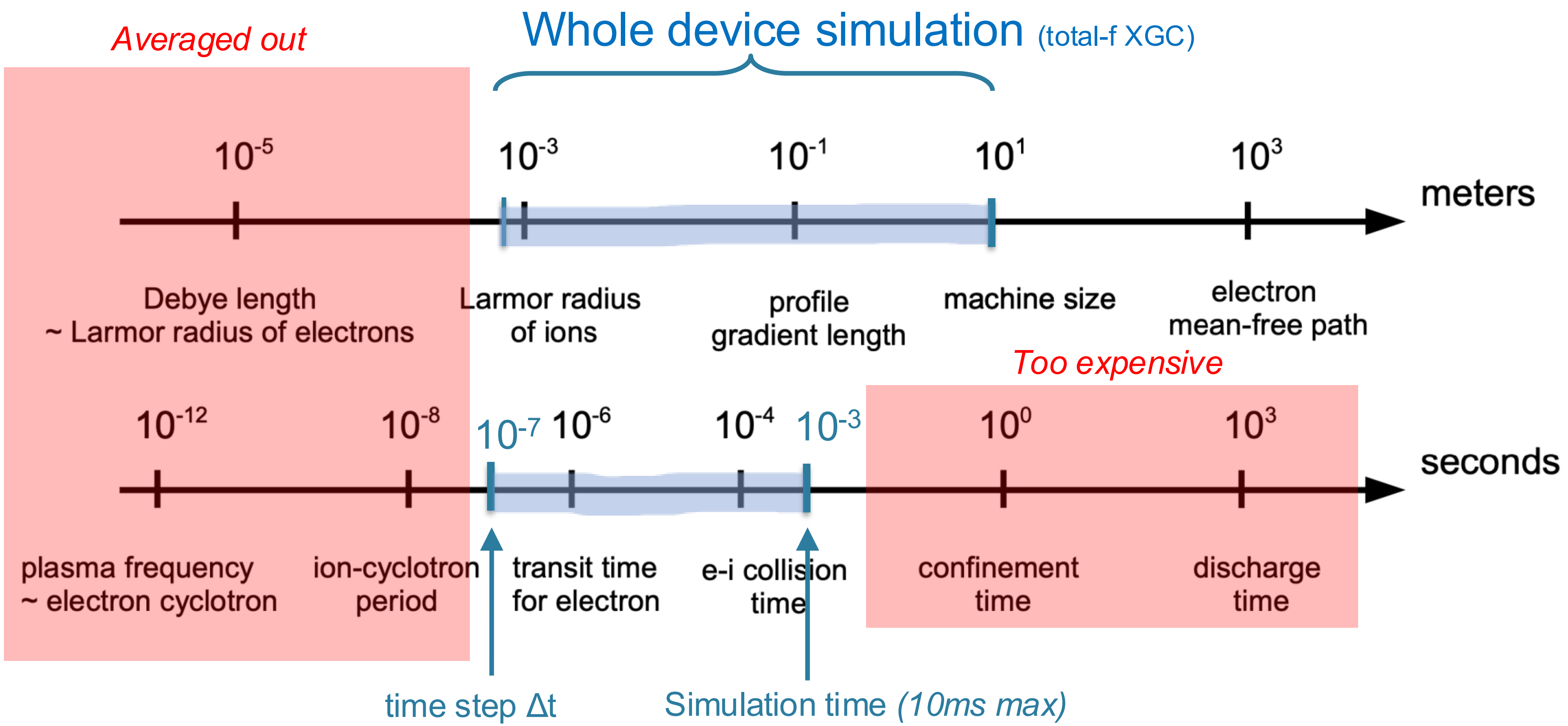

The gyrocentre distribution function f is evolved with the 5D gyrokinetic equation

Gyromotion is reduced

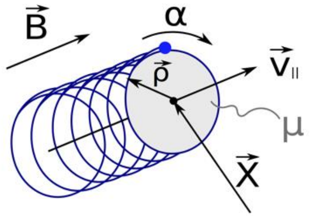

$x = X + \rho$
$\dot{\mu} = 0$

$$\frac{\partial f}{\partial t} + \dot{\boldsymbol{X}}[\phi] \cdot \frac{\partial f}{\partial \boldsymbol{X}} + \dot{v}_{\parallel}[\phi] \frac{\partial f}{\partial v_{\parallel}} = \mathcal{C}[f] + \mathcal{S} \tag{1}$$

$$\dot{\boldsymbol{X}} = v_{\parallel}\boldsymbol{b} + \left(\boldsymbol{v}_{\nabla B} + \boldsymbol{v}_k + \boldsymbol{v}_{E\times B}\right) B/B_{\parallel}^{*}, \tag{2}$$

$$\dot{v}_{\parallel} = -\dot{\boldsymbol{X}} \cdot \left(\mu \nabla B + q\nabla\langle\phi\rangle\right)/m v_{\parallel}. \tag{3}$$

The consistent electrostatic potential is solved with a quasi-neutrality equation

$$-\sum_s \nabla_{\perp} \frac{m n_s}{e B^2} \nabla_{\perp}\phi = \sum_s Z_s \int_{-\infty}^{+\infty} dv_{\parallel} \int_0^{+\infty} d\mu \oint d\alpha\, f_s(\boldsymbol{x} - \boldsymbol{\rho}, v_{\parallel}, \mu). \tag{4}$$

Delta-f and total-f representations

The delta-f representation $f = f_0 + \delta f$ evolves the delta-f gyrokinetic equation

$$\frac{\partial \delta f}{\partial t} + \dot{\boldsymbol{X}}[\phi] \cdot \frac{\partial \delta f}{\partial \boldsymbol{X}} + \dot{v}_{\|}[\phi] \frac{\partial \delta f}{\partial v_{\|}} = -\boldsymbol{v}_{E\times B} \cdot \nabla f_0 + \mathcal{C}[\delta f] + \mathcal{S} \quad (5)$$

f0 is a fixed Maxwellian (delta-f)

Delta-f and total-f representations

The delta-f representation $f = f_0 + \delta f$ evolves the delta-f gyrokinetic equation

$$\frac{\partial \delta f}{\partial t} + \dot{\mathbf{X}}[\phi] \cdot \frac{\partial \delta f}{\partial \mathbf{X}} + \dot{v}_{\parallel}[\phi] \frac{\partial \delta f}{\partial v_{\parallel}} = -\mathbf{v}_{E\times B} \cdot \nabla f_0 + \mathcal{C}[\delta f] + \mathcal{S} \tag{5}$$

f0 is a fixed Maxwellian (delta-f)

The total-f representation $f = f_0(t) + \delta f$ keeps the background term and accounts for full nonlinear collisions

$$\frac{\partial \delta f}{\partial t} + \dot{\mathbf{X}}[\phi] \cdot \frac{\partial \delta f}{\partial \mathbf{X}} + \dot{v}_{\parallel}[\phi] \frac{\partial \delta f}{\partial v_{\parallel}} = -\dot{\mathbf{X}} \cdot \nabla f_0 + \mathcal{C}[f_0 + \delta f] + \mathcal{S} \tag{6}$$

The delta-f representation $f = f_0 + \delta f$ evolves the delta-f gyrokinetic equation

$$\frac{\partial \delta f}{\partial t} + \dot{\boldsymbol{X}}[\phi] \cdot \frac{\partial \delta f}{\partial \boldsymbol{X}} + \dot{v}_{\parallel}[\phi] \frac{\partial \delta f}{\partial v_{\parallel}} = -\boldsymbol{v}_{E\times B} \cdot \nabla f_0 + \mathcal{C}[\delta f] + \mathcal{S} \quad (5)$$

f0 is a fixed Maxwellian (delta-f)

The total-f representation $f = f_0(t) + \delta f$ keeps the background term and accounts for full nonlinear collisions

$$\frac{\partial \delta f}{\partial t} + \dot{\boldsymbol{X}}[\phi] \cdot \frac{\partial \delta f}{\partial \boldsymbol{X}} + \dot{v}_{\parallel}[\phi] \frac{\partial \delta f}{\partial v_{\parallel}} = -\dot{\boldsymbol{X}} \cdot \nabla f_0 + \mathcal{C}[f_0 + \delta f] + \mathcal{S} \quad (6)$$

$$f(t) := f_0(t) + \widetilde{\delta f}$$

f_{grid} or Maxwellian(t) ← $f_0(t)$; $\widetilde{\delta f}$ → PIC

Relaxation:
$$\begin{cases} f_0 := f_0 + \alpha \left(\widetilde{\delta f}\right)^{(n=0)} \\ \widetilde{\delta f} := \widetilde{\delta f} - \alpha \left(\widetilde{\delta f}\right)^{(n=0)} \end{cases}$$

Total-f scheme: [Ku et al. J. Comp. Phys. (2016)]

Background term $\dot{X}_0 \cdot \nabla f_0$

- The background term $\dot{X}_0 \cdot \nabla f_0$ drives a large initial transient if using a local Maxwellian background $f_0 = f_{loc}(\psi, \varepsilon, \mu)$

- It's not the case with a canonical Maxwellian background $f_0 = f_{can}(p_\varphi, \varepsilon, \mu)$.

Note that the total-f collision-less part of the weight evolution equation is computed along characteristics with the "direct delta-f scheme"

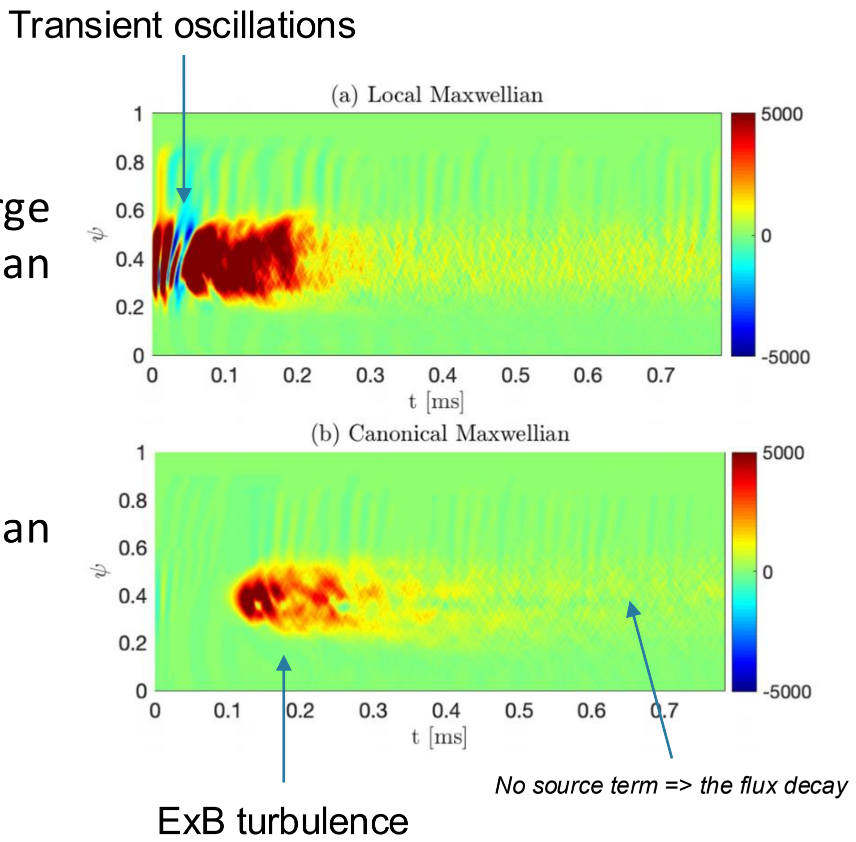

Angelino et al. *Phys. of Plasmas* 13 (2006)
Trivedi, Dominski et al. *Phys. Plasmas* (2024)

2. WDM by coupling delta-f and total-f models

We implemented a model where core and edge regions use the same equations but different background f_0 [Trivedi, Dominski et al. *Phys. Plasmas* (2024)]

$$f_0 = \varpi\, f_{can} + (1 - \varpi) f_{loc}$$

The canonical background term $\dot{X}_0 \cdot \nabla f_{can}$ being small we can use a Krook term on the RHS that keeps the temperature profile fixed, without continuously exciting transient GAM like oscillations.

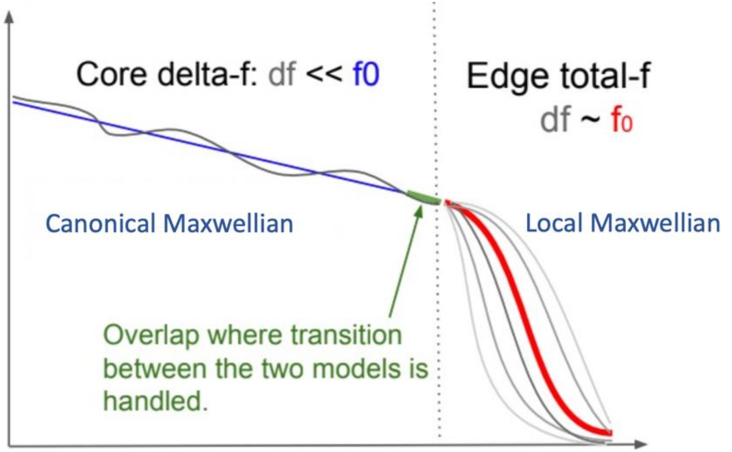

Core	Gradient driven	Thermal-bath	Fixed background f_0	Canonical Max. f_0
Edge	Flux driven	Core fluxes and Neutral recycling	Relaxing background f_0 (t)	Local Maxwellian f_0

Local and global approaches

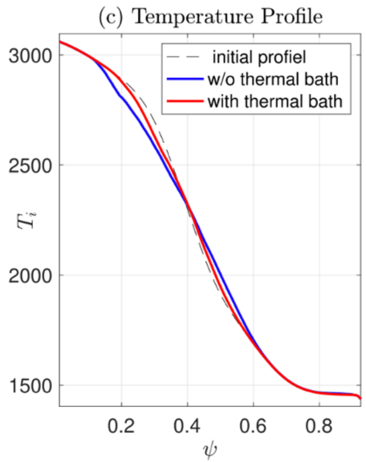

Global models include radial profiles of n_0, T_0, … in a Maxwellian

- Flux-driven: the profiles evolves with respect to source profiles (c.f. edge)
- Gradient-driven: Krook-like terms maintain the profiles (c.f. core)

Local models use fixed background (n_0, T_0) and gradients $(a/L_n, a/L_T)$

- Computations are done on a surface
  - gyrokinetic: GKW, GX, GENE,…
  - neoclassic: NEO, FACIT
- The background profiles can be evolved iteratively with a transport model
  - Multiple simulations needed for covering multiple surfaces and multiple time steps
  - Tungsten example with FACIT and $\frac{dn}{dt} + \nabla \cdot \mathbf{\Gamma} = S_{atom}$

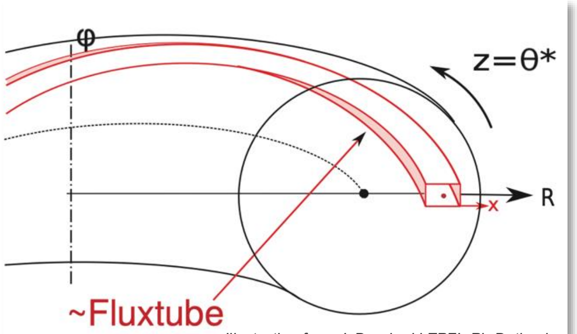

Illustration from J. Dominski EPFL Ph.D. thesis

Plasma scales and relevance of gyrokinetic

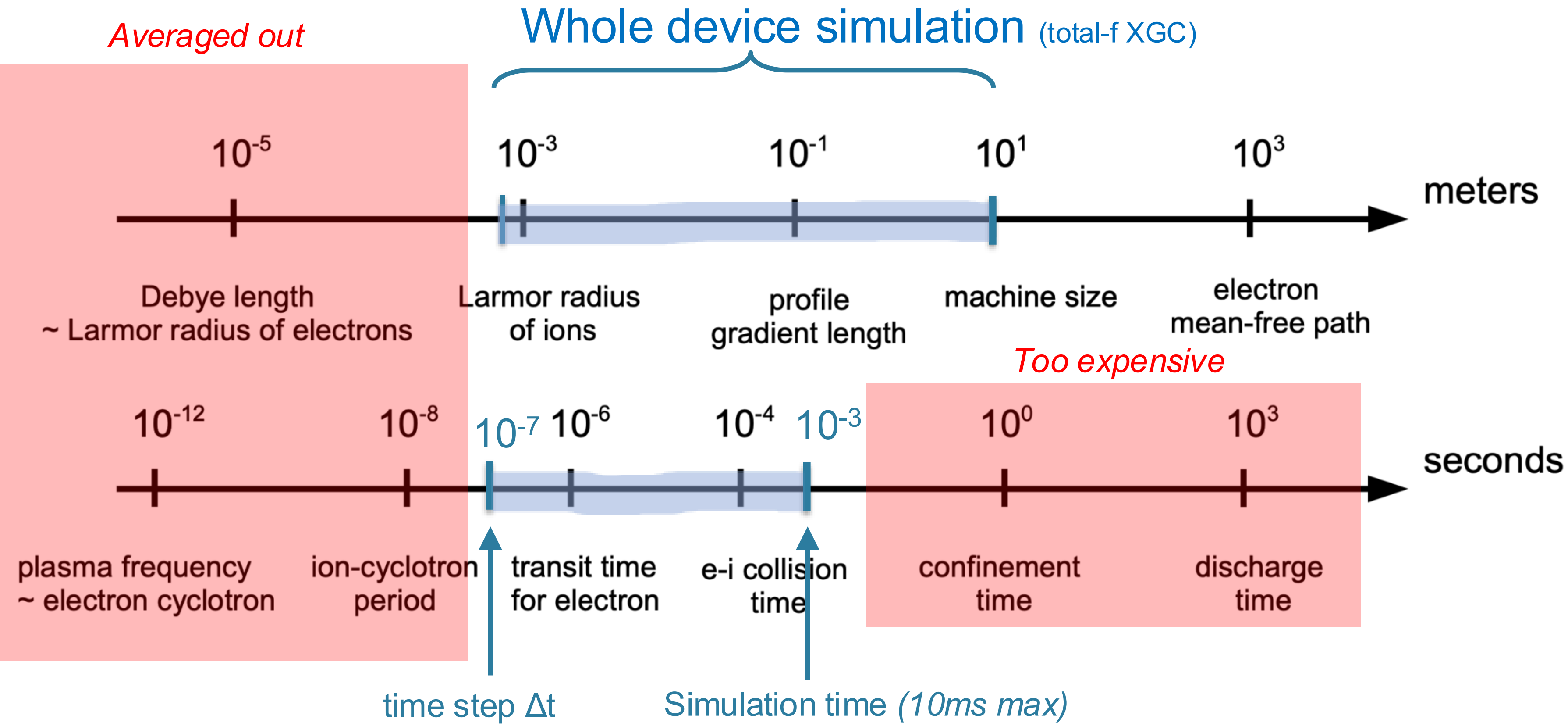

Plasma scales and relevance of gyrokinetic

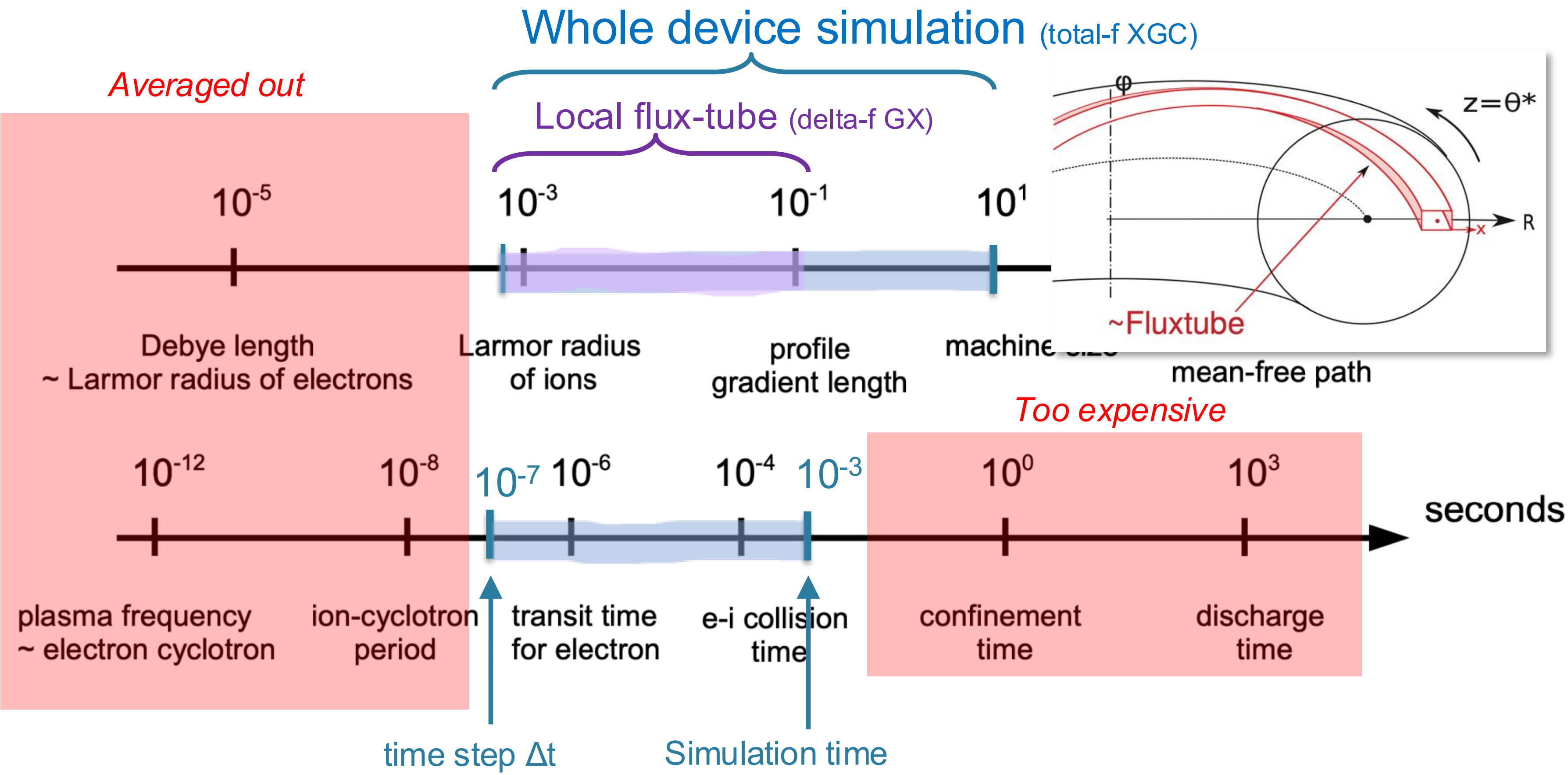

Plasma scales and relevance of gyrokinetic

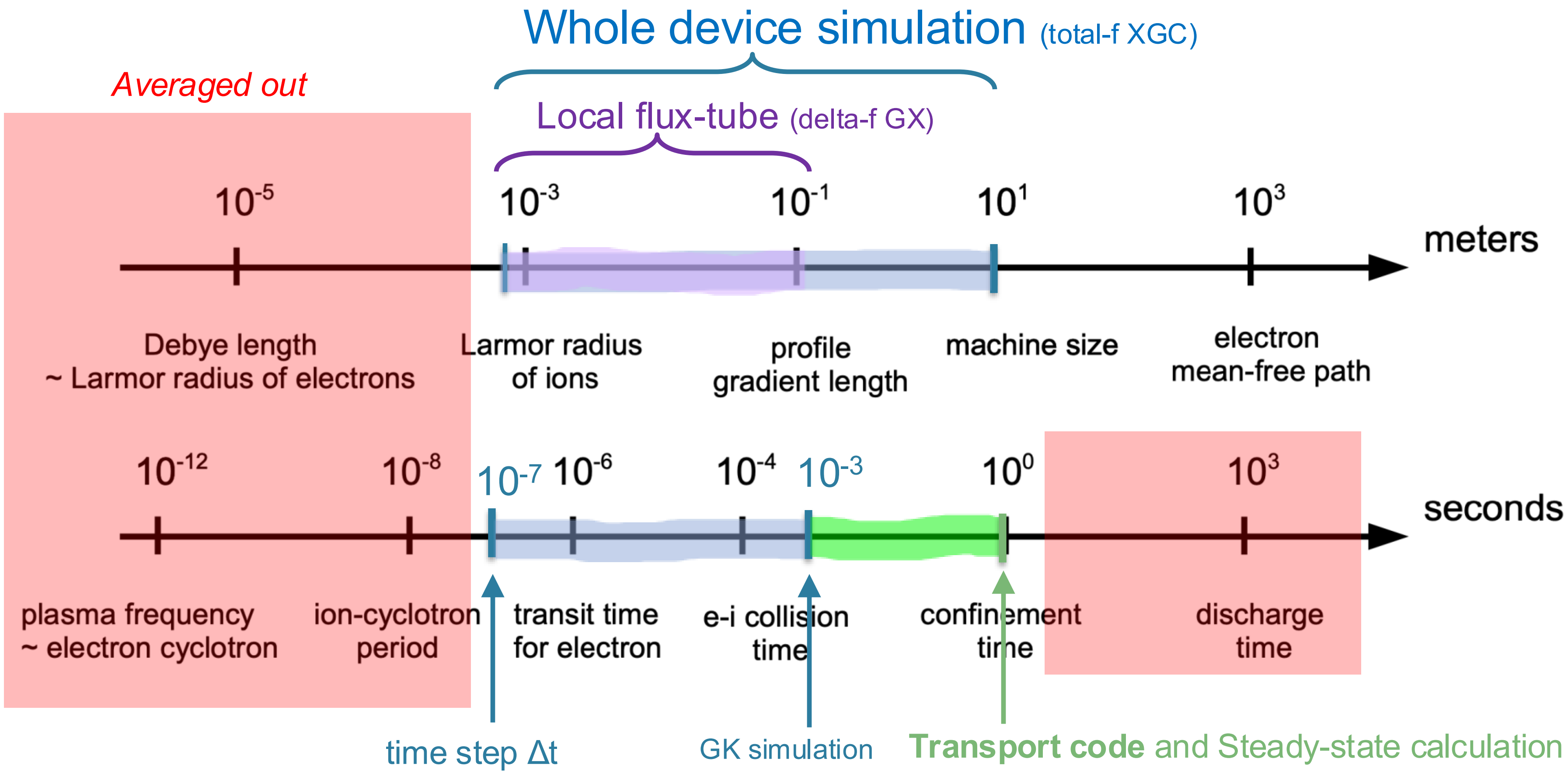

GK provides the transport driven by the input profiles
Transport code evolves these profiles consistently with the transport

3. Balance between heat source, transport, and radiation

Core δf informed with profiles from experiment or gyrokinetic -transport models

- GENE-Tango, GX-T3D, XGC-equation free, XGC-Tango,…

For a more accurate modeling of the edge physics and pedestal shape prediction, impurities are being modeled gyrokinetically with their atomic physic interactions (ADAS). The sink of energy due their radiation would then be incorporated in the transport code.

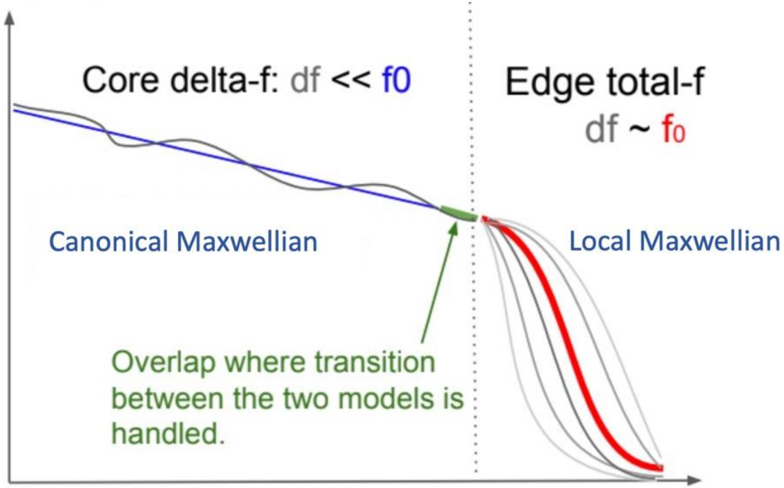

Acts as a heat source for the edge

Radiation + transport

Application: modeling tungsten and low-Z impurity transport in tokamaks

- WEST: tungsten nitrogen interaction
- Atomic physics: modeling the various tungsten ions
- Application to ASDEX-U H-mode simulations

Motivation

Tungsten is sputtered from the wall and contaminates the plasma, where it radiates a significant fraction of the input power. Not only the divertor, but also the wall of ITER will be in tungsten

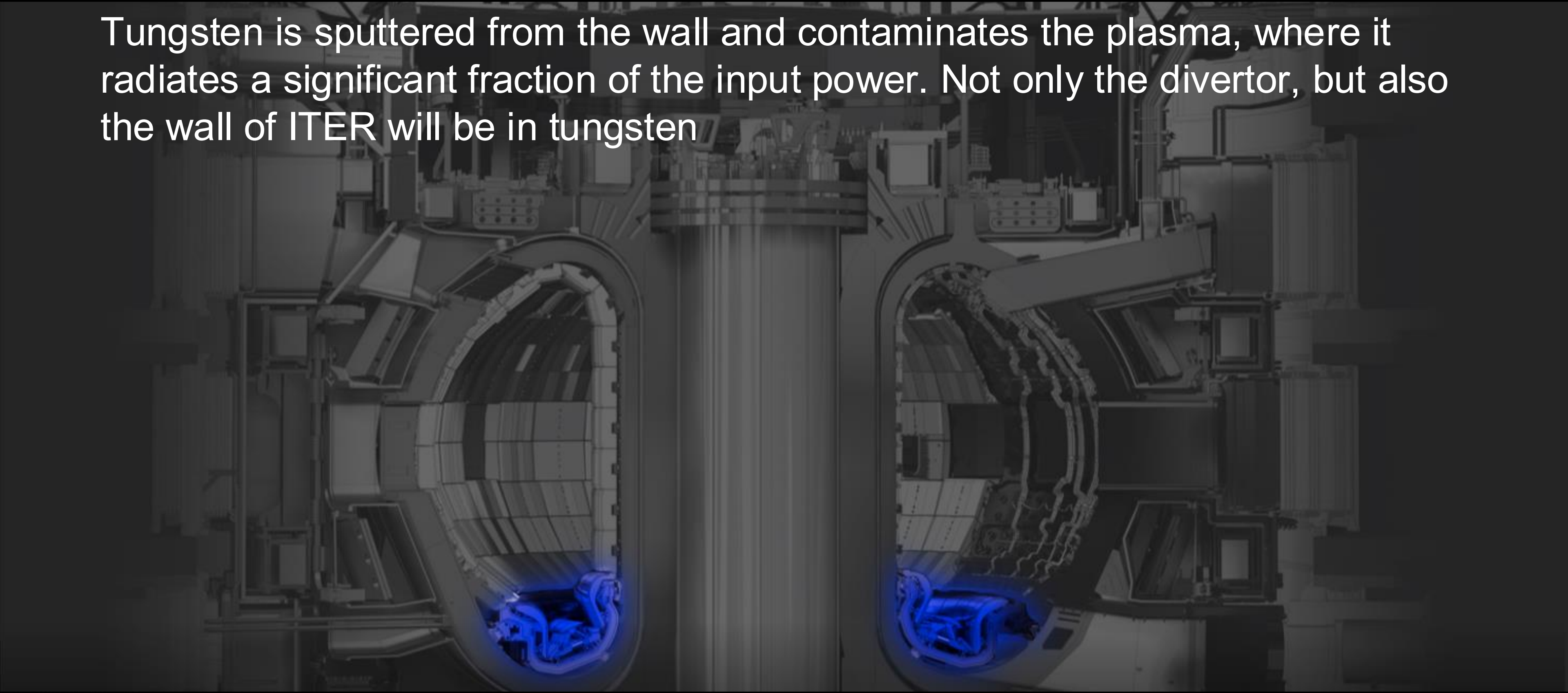

Motivation

Tungsten is sputtered from the wall and contaminates the plasma, where it radiates a significant fraction of the input power. Not only the divertor, but also the wall of ITER will be in tungsten

WEST is a test bed for ITER (divertor and wall)

- Ramp-up phase has no temperature screening and a large cooling rate (cold and hot branches)
- Light impurity seeding (N) increases the core temperature during the ramp-up phase [Maget PPCF (2022)]
- Boron reduces tungsten sputtering (GDB & IPD)
- Radiative collapse
- …

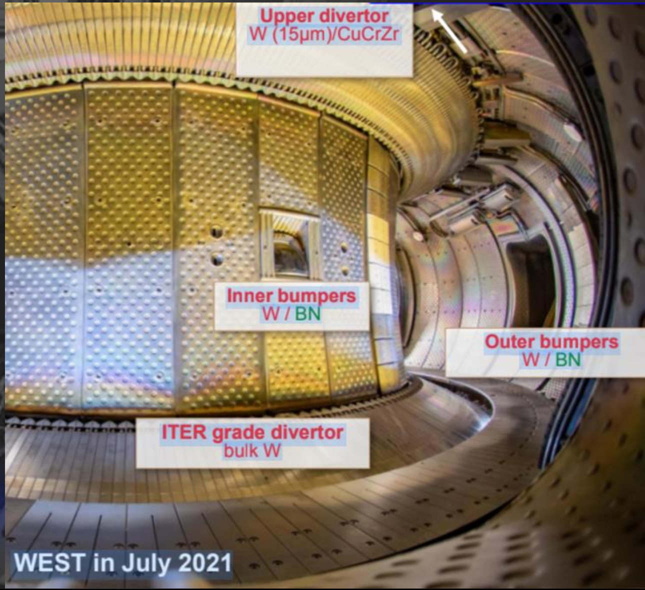

Dominski et al. 2024 Nucl. Fusion in press https://doi.org/10.1088/1741-4326/ad8c63

Collisional tungsten W^{25+} transport in the core is altered by nitrogen N^{7+}

(a) Nitrogen reduces the tungsten penetration.

(b) Reduction of the neoclassical peaking in presence of 2.5% of nitrogen (steady-state calculation).

If $\Gamma = 0$ then $\boldsymbol{\nabla \ln n = V/D}$, given that $\Gamma = V\,n\, - D\,\nabla n$

FACIT: compute local D and V coefficients directly

XGC: Scan many radial profiles of density gradient (green dashed lines) and interpolate the gradient giving $\Gamma = 0$

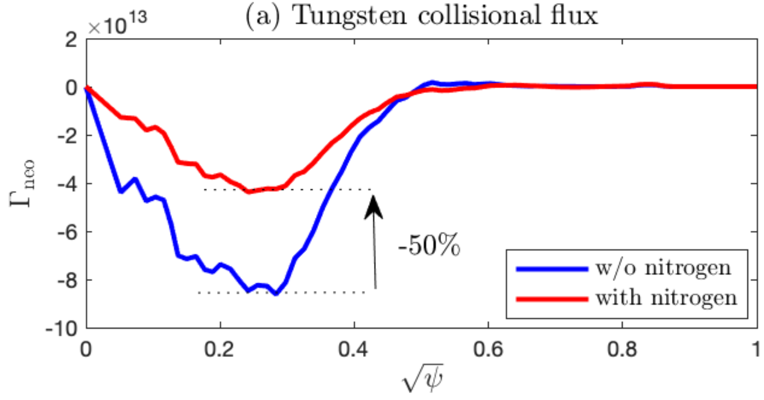

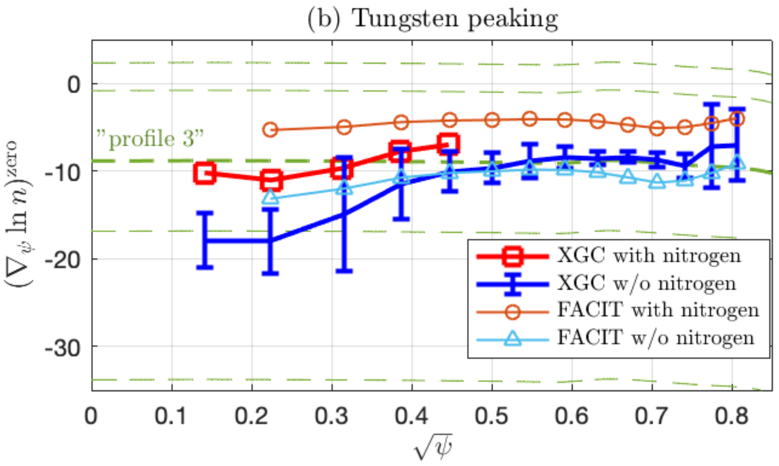

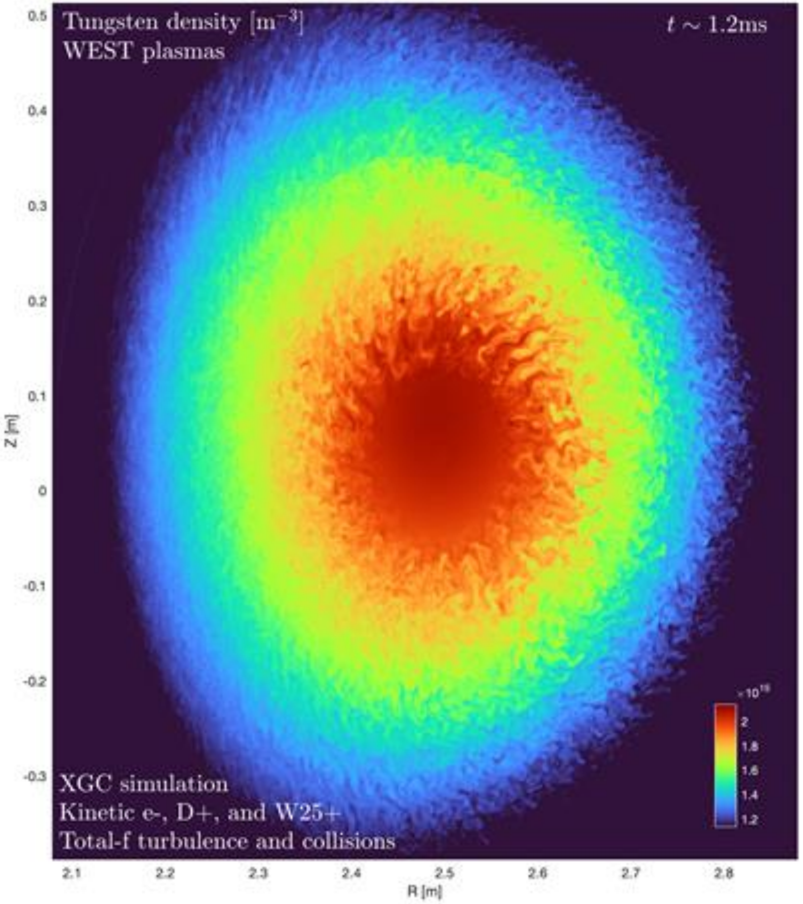

This is the **core tungsten density** (up to $\sqrt{\psi}\approx 0.9$)

- **Large turbulent fluctuation** ~30% of background
- Near axis dominated by **collisional peaking V/D**
- **Tungsten screening** at mid-radius: increase of D.
- **Nitrogen stabilizes** turbulence and reduce this screening

Nitrogen impurities stabilize turbulence (and the linear micro instability drive)

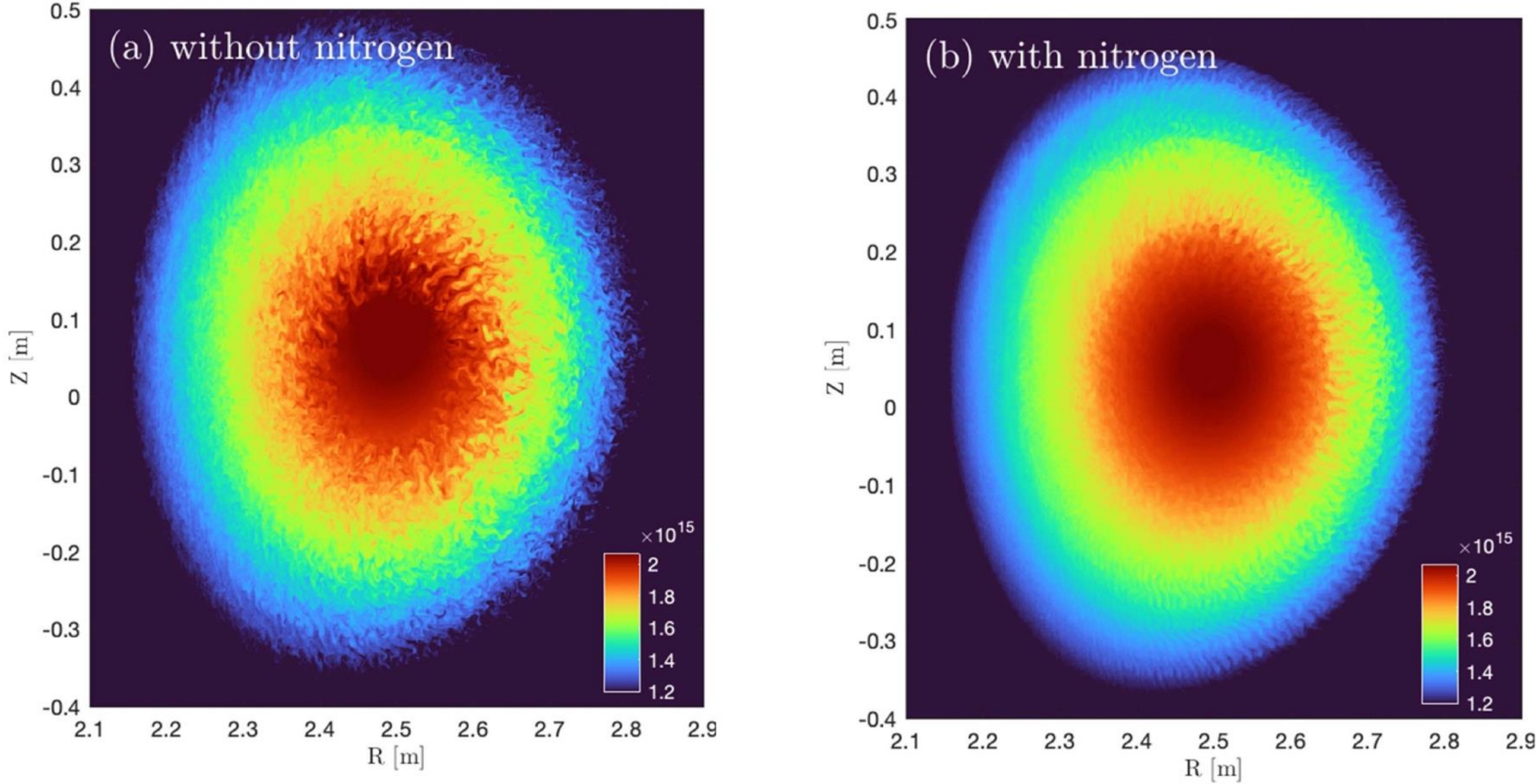

Dominski et al. 2024 Nucl. Fusion in press https://doi.org/10.1088/1741-4326/ad8c63

The region of neoclassical peaking is enlarged by the presence of nitrogen that stabilizes turbulence. In turn, more nitrogen accumulates near axis (cn=2.5%).

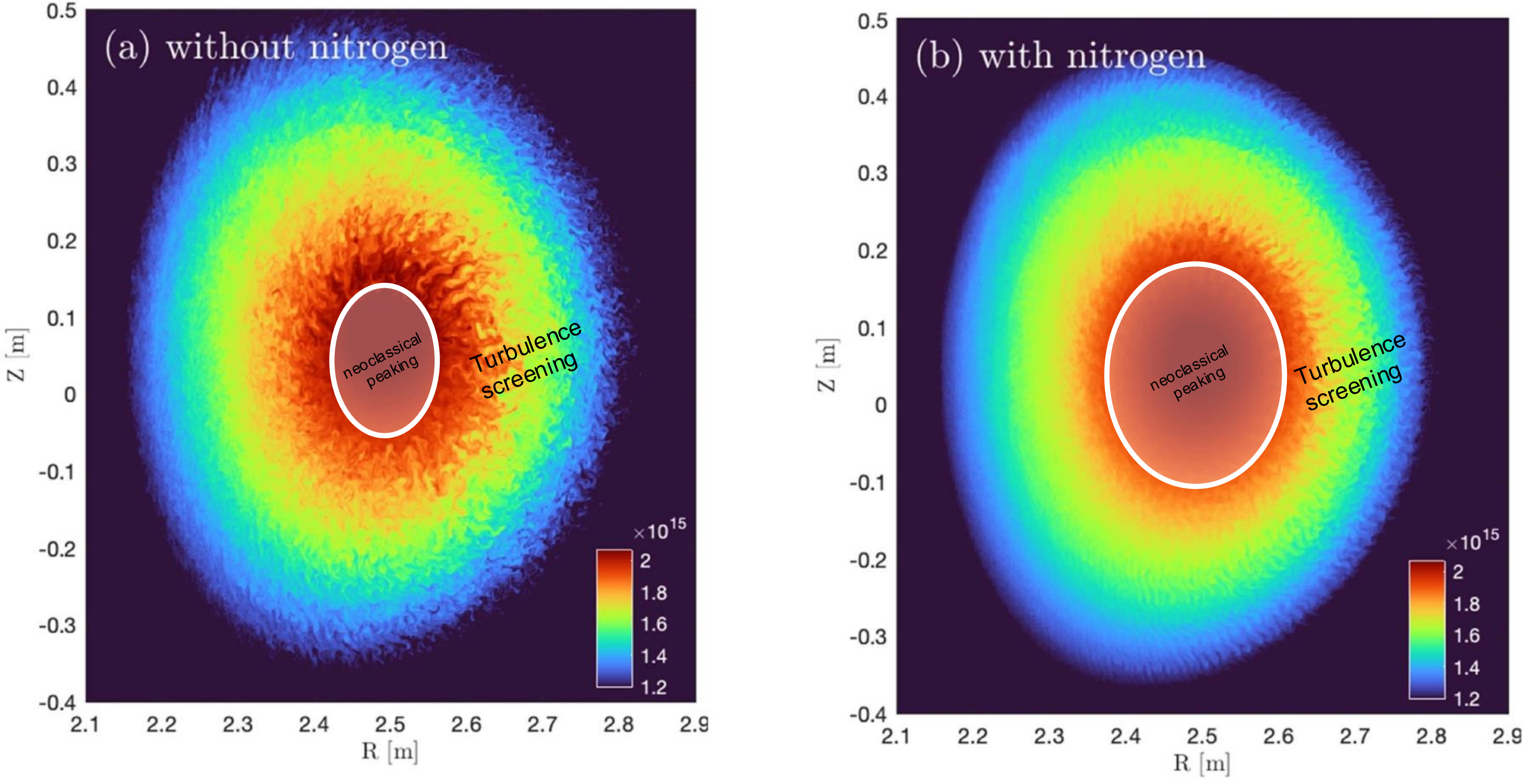

Dominski et al. 2024 Nucl. Fusion in press https://doi.org/10.1088/1741-4326/ad8c63

Dominski et al. 2024 Nucl. Fusion in press https://doi.org/10.1088/1741-4326/ad8c63

Using multiple gyrokinetic simulations, we compute the profile of tungsten gradient leading to a zero particle flux.

(a) We integrate it to obtain a profile of tungsten density.
(b) We use a synthetic diagnostic of radiation power measured by bolometers. [Devynck et al 2021 JPC]

Including nitrogen is necessary for an accurate prediction.

Nitrogen increases the predicted tungsten accumulation on axis.

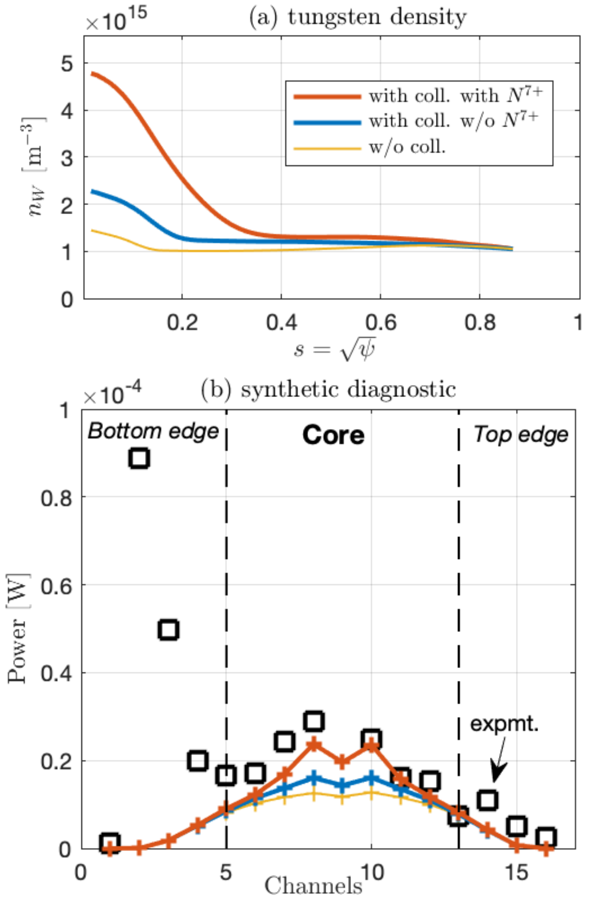

Dominski et al. 2024 Nucl. Fusion in press https://doi.org/10.1088/1741-4326/ad8c63

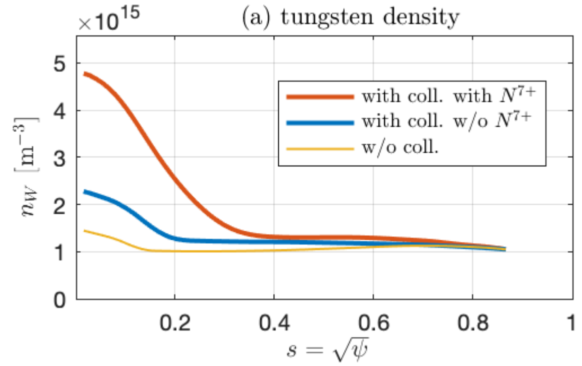

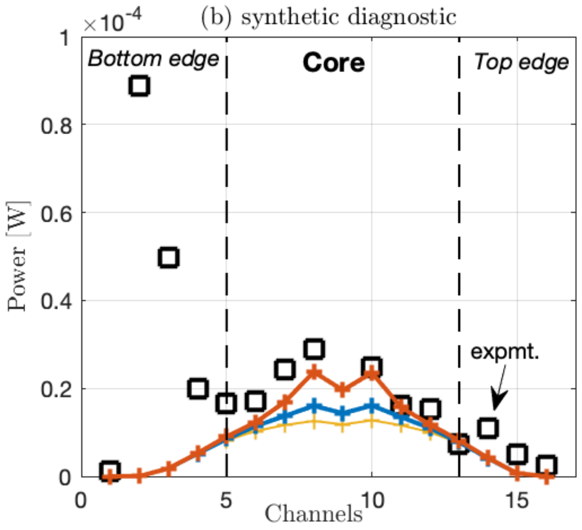

Intermediate conclusion:

- This finding is important for the plasma current ramp-up phase of ITER, where light impurities seeding will be desirable to achieve low temperatures at the plasma-facing components.
- It provides further argument for applying early ECRH heating to maintain margins on the core power balance.

2. WEST CEDA – coupling transport and atomic physics

Given the importance of the collisional peaking near axis, a new reduced model including all tungsten ions is being developed.

$$\frac{dn_j}{dt} = \nabla.\Gamma_j + \sigma_{j-1} n_{j-1} - (\sigma_j + \alpha_j) n_j + \alpha_{j+1} n_{j+1}$$

Neoclassical transport of all W ions with **FACIT**, can include nitrogen impurities.

Ionization/recombination between W ions with **ADAS** rates, and for radiation.

Use a fixed boundary condition at the outer edge and evolve the density profiles of all tungsten ions from this continuity equation.

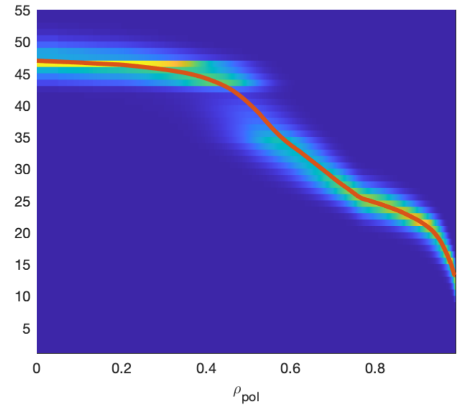

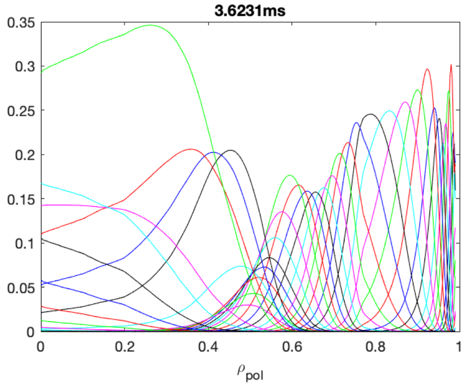

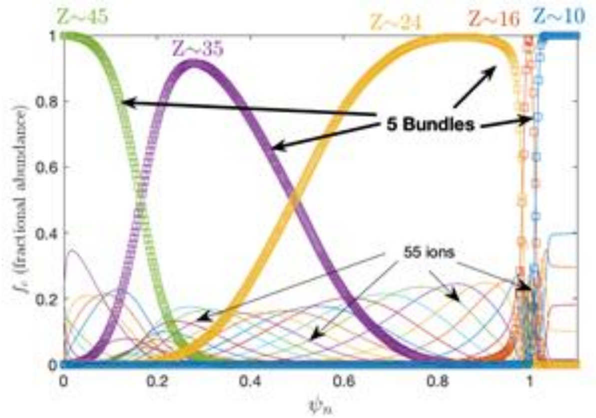

- The many charge states of tungsten ions are modeled with a few **gyrokinetic bundles**

Fractional abundance is computed from atomic balance between ionization and recombination using **ADAS rates**.

$$\frac{dn_i}{dt} = \sigma_{i-1}n_{i-1} - (\sigma_i + \alpha_i)n_i + \alpha_{i+1}n_{i+1}$$

- **Tungsten radiations** are also computed with **ADAS rates**.

$$P_{\rm rad} = n_e n_{\rm w}\ L_{\rm cool}$$

The cooling factor is consistently modeled with all ionization states.

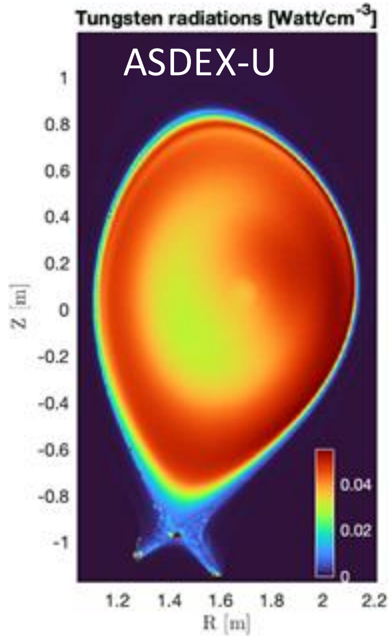

Collaboration with M. O'Mullane (UKAEA) and the ADAS group.

Previous bundling from Coronal approximation: Dominski et al. *Phys. Plasmas* (2024)

3. Bundle verification profiles computed over ADAS

- We let the tungsten ions/bundles reach atomic balance, and we compare bundles and the ions they represent

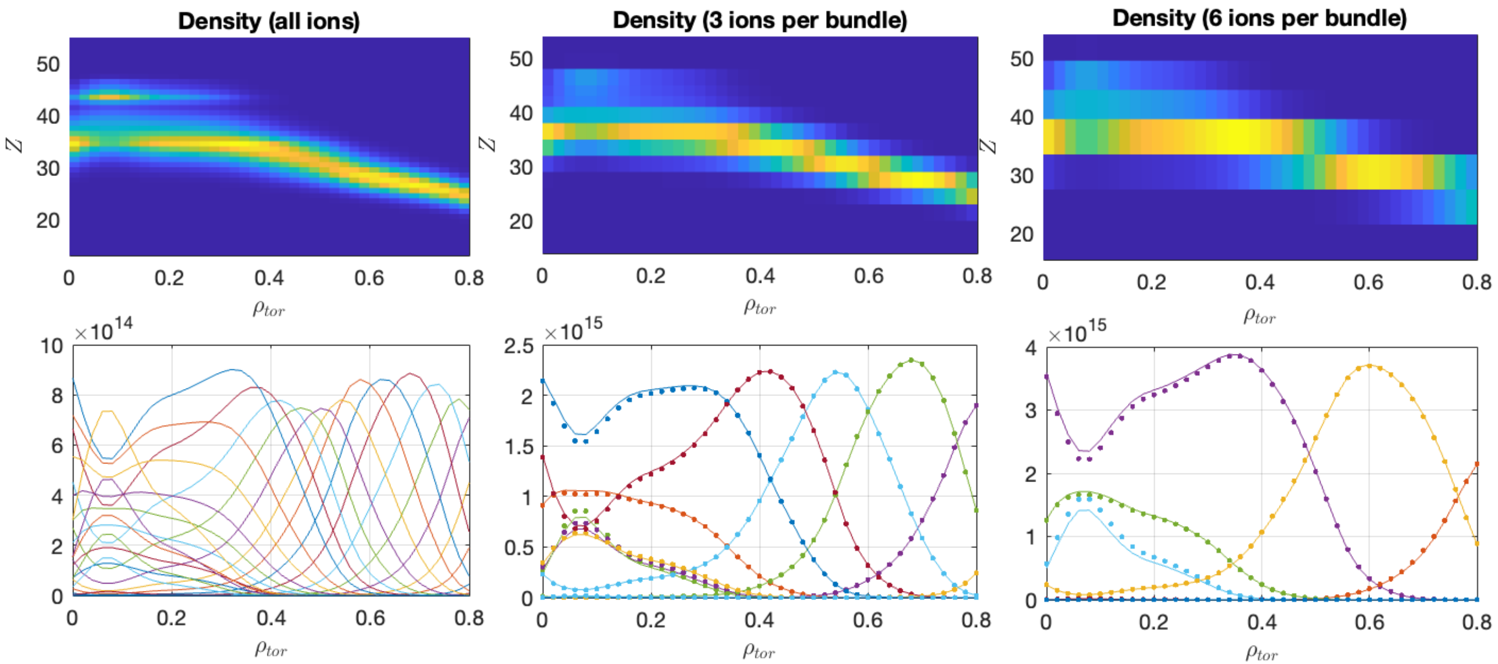

4. AUG - collision and turbulence simulations (t~1.5ms)

- No rotation
- Private region saturated in impurities
- Tungsten penetrates at separatrix because of collisions and density asymmetry. Confirmed in simulation with tungsten bundles.

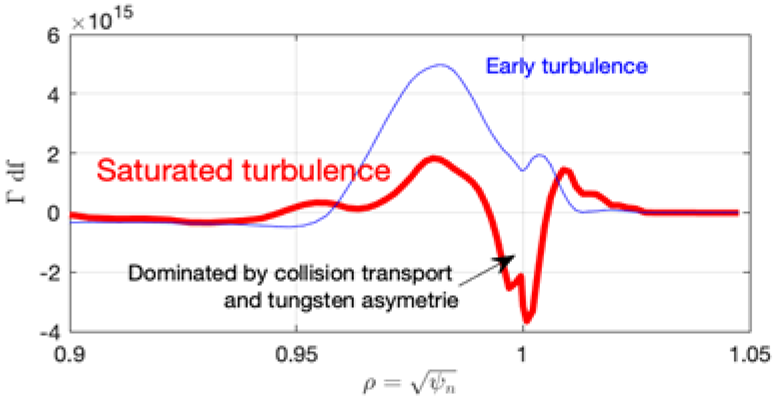

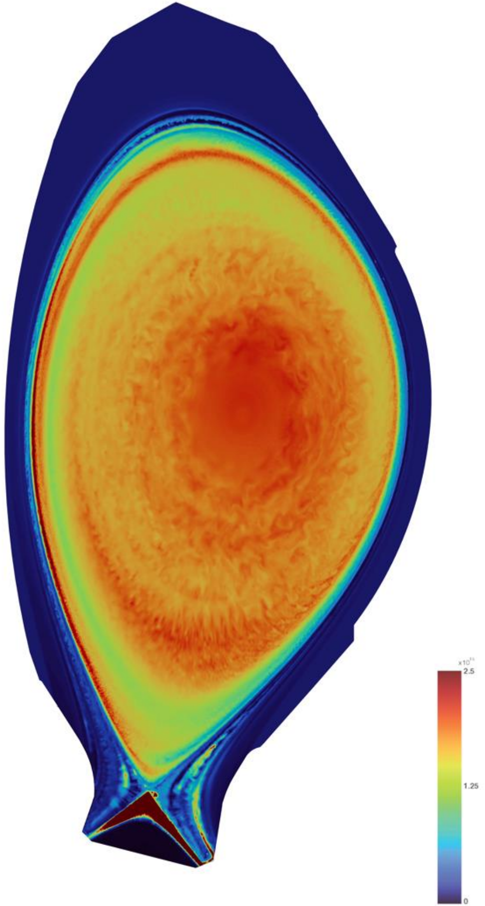

4. AUG – Influence of rotation (T~2.5ms)

Collaboration with A Kallenbach, E Viezzer, and AUG team

- Focus our modeling on the edge.

  - Bundle Z=24, core to pedestal top (see figure)

  - Bundle Z=12, pedestal foot to wall.

- Include rotation and light impurities of Boron.
- Collisional penetration of tungsten at separatrix.
- Accumulation of W at high field side in the pedestal. *Similar high field side accumulation of tungsten in AUG observed by Korving et al. Phys. Plasmas 31, 052504 (2024)*

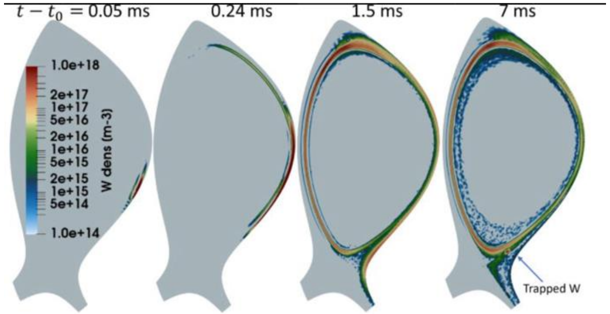

Up-down asymmetries in PS regime w/o rotation: Dominski JPP (2019) simulations; P. Helander PoP (1998) theory

Asymmetries in a non-rotating model JET plasma pedestal: Dominski et al. Phys. Plasmas (2024)

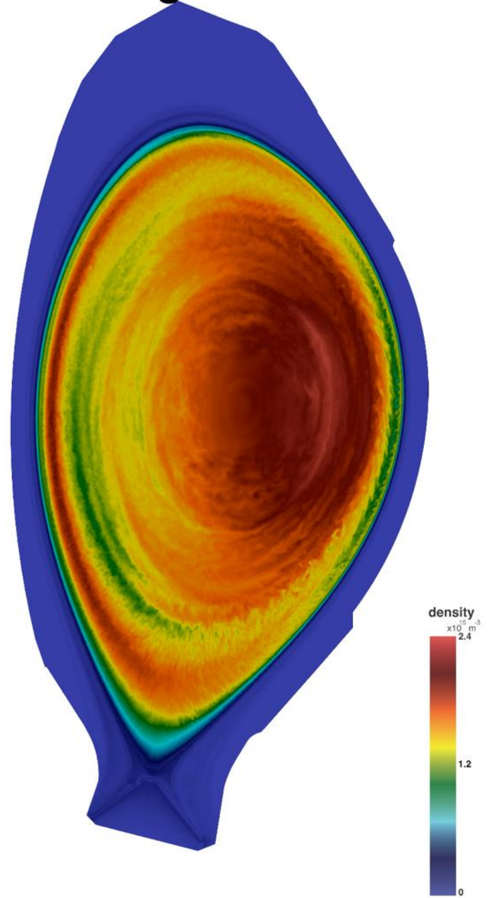

Conclusion

- Prediction of the steady tungsten peaking in WEST
  - Influence of nitrogen n^{7+}
  - Validation with a synthetic diagnostic of bolometry
- New model for all W ions transport and atomic physics
  - Studying the formation of off-axis bump of tungsten and radiation
  - Interest in adding local turbulent transport
- Tungsten bundles with atomic physics
  - Ionization/recombination and radiations
  - KinBL a library for atomic calculation on CPU and GPU (Kokkos)
- H-mode saturated turbulence in whole device of ASDEX-U
  - Interplay between collisional and turbulent transport
  - Penetration of tungsten at separatrix
- Modeling effort towards the wall
  - Next: tungsten ions/bundles in SOL with sources

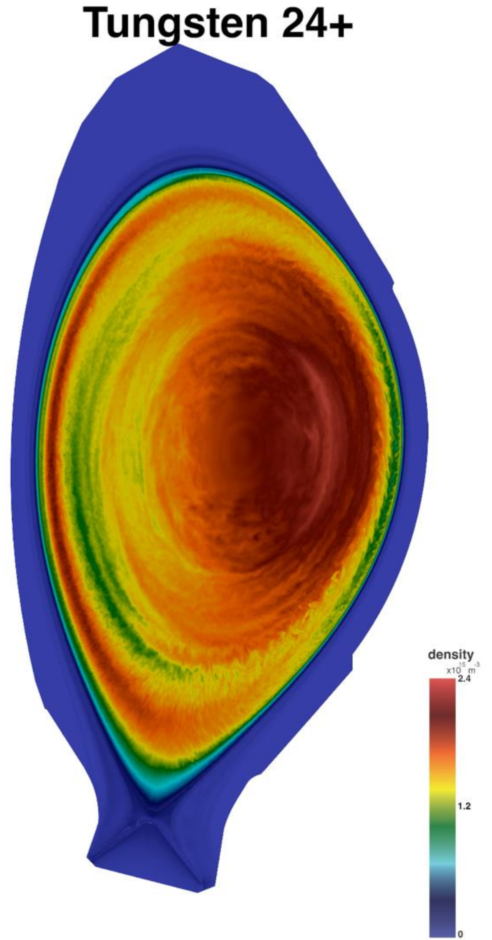

Backup slides

A. Core-edge kinetic coupling algorithm

1. A **blended particle distribution function** is used

$$\check{f} = \varpi\, f^{\mathrm{Core}} + (1-\varpi)\, f^{\mathrm{Edge}}$$

2. The **fields' equations** (Poison and Ampere) are coupled at the level of their source term, with for example

$$\mathcal{L}\check{\phi} = \bar{n}^{\mathrm{Core}} + \bar{n}^{\mathrm{Edge}}$$

3. **Buffer regions** are used after the overlap to provide a correct information in the overlap.

Necessary and suff. condition: $\left(f^{\mathrm{Core}} - f^{\mathrm{Edge}}\right)\left(\dot{X}\cdot\dfrac{\partial\varpi}{\partial X}\right) = 0$

4. The buffers need to be updated for long simulations or when a heat source is used in the core, by **coupling the particle distribution function** (f-coupling).

Example: f-coupling of the core buffer

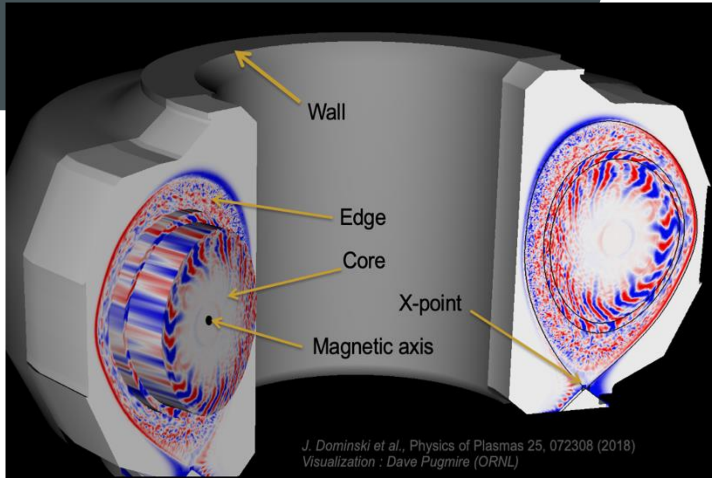

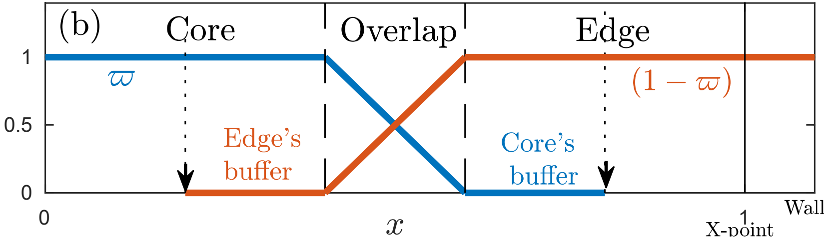

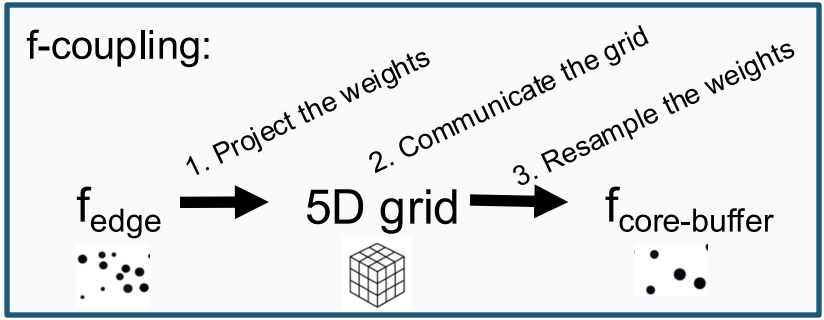

Dominski et al. *Phys. Plasmas* (2018)
Dominski et al. *Phys. Plasmas* (2021)

B. Gyrokinetic bundles modeled with finite elements, and a Coronal approximation (Without ADAS rates)

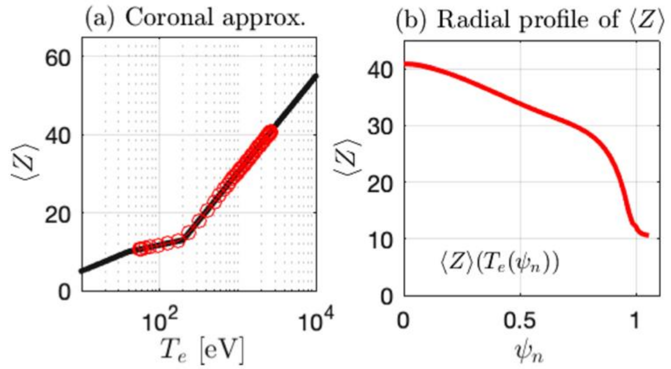

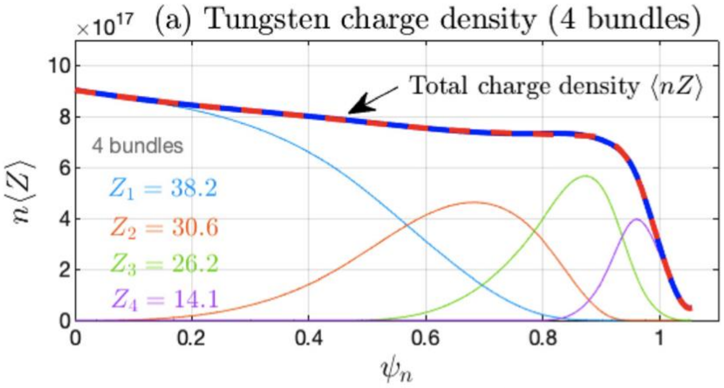

- A Coronal approximation is used to determine <Z> as a function of T_e. **It was before I use ADAS atomic physics.**

- The density and charge are represented with finite elements (bsplines).

$$n(\psi_n) = \sum_i c_i \Lambda_i(\psi_n)$$

$$\langle nZ \rangle(\psi_n) = \sum_i c_i Z_i \Lambda_i(\psi_n)$$

- The system is solved with a weak formulation.

$$\begin{cases} c_i = (M^{-1})_{ij} \int d\psi \, \Lambda_j(\psi) \, \dfrac{\langle nZ \rangle(\psi)}{\langle Z \rangle(\psi)}, \\ c_i Z_i = (M^{-1})_{ij} \int d\psi \, \Lambda_j(\psi) \, \langle nZ \rangle(\psi), \end{cases}$$

$$M_{ij} = \int d\psi \, \Lambda_i(\psi) \Lambda_j(\psi)$$

Dominski et al. *Phys. Plasmas* (2024)

- Recent study of tungsten collisional transport using **4 bundles of tungsten**
- Influence of **large asymmetries** on the **collisional transport in the edge**
  - Reversal of the asymmetry in the edge caused by ion orbit-loss effects and $E_{||}$
  - Reversal of flux → accumulation in the pedestal top

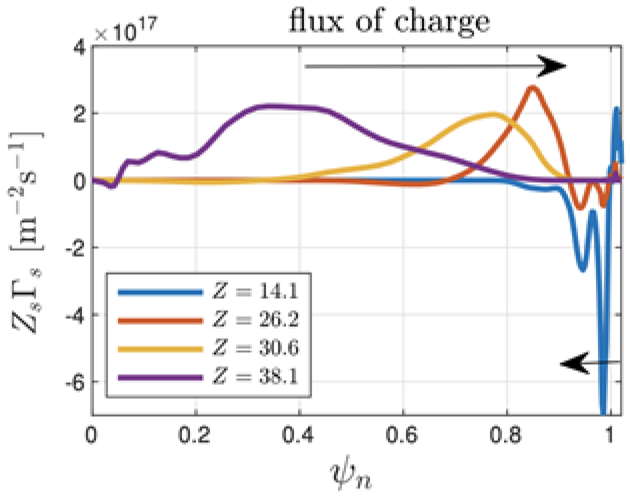

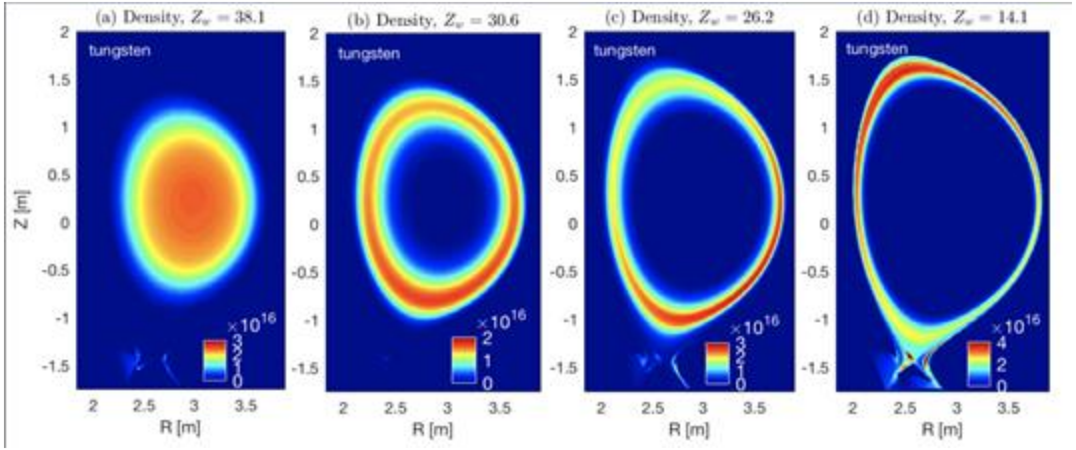

Dominski et al. *Phys. Plasmas* (2024)

When the dominant up-down asymmetry cancels, the in-out asymmetry rise.

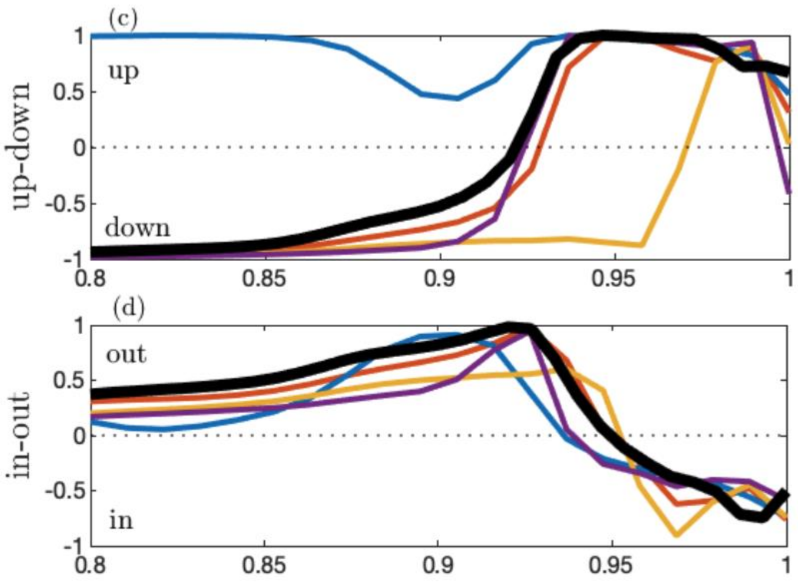

Reversal of the asymmetry in the edge is caused by ion orbit loss and $E_{||}$

$$\nabla_{||} \ln n_w \simeq \frac{eZ}{T_w} E_{||} + \frac{1}{n_w T_w} R_{||,w}$$

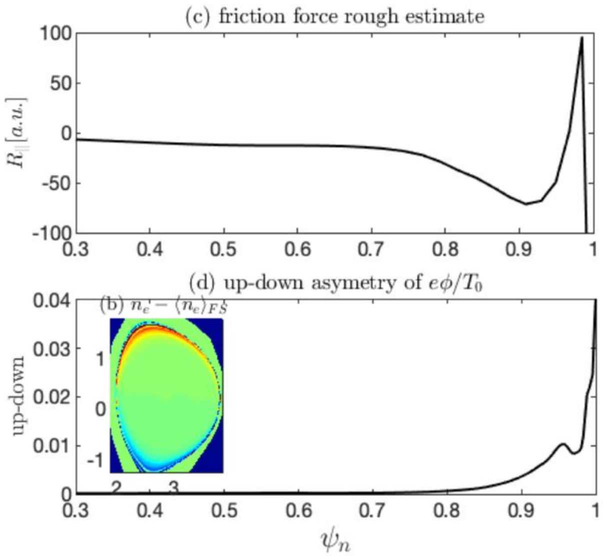

Dominski et al. *Phys. Plasmas* (2024)